DOI: 10.1070/RCR4878

Hybrid materials based on graphene derivatives and porphyrin metal-organic frameworks

Vladimir V. Arslanov,[a*] Maria A. Kalinina,[a] Elizaveta V. Ermakova,[a] Oleg A. Raitman,[a] Yulia G. Gorbunova,[b] Oleg E. Aksyutin,[c] Alexander G. Ishkov,[c] Vladimir A. Grachev,[a] Aslan Yu. Tsivadze [a]

[a] A.N.Frumkin Institute of Physical Chemistry and Electrochemistry, Russian Academy of Sciences, Leninsky prosp. 31, korpus 4, 119071 Moscow, Russian Federation
[b] Kurnakov Institute of General and Inorganic Chemistry, Russian Academy of Sciences, Leninsky prosp. 31, 119991 Moscow, Russian Federation
[c] Public Joint Stock Company Gazprom, ul. Nametkina 16, 117997 Moscow, Russian Federation

Domestic and foreign literature on methods for obtaining graphene and its derivatives [graphene oxide (GO) and reduced GO] as representatives of the family of 2D layered materials is analyzed. Particular attention is paid to GO. Great potential of post-synthetic modification as well as unique properties of the material and its derivatives make them promising for a variety of applications including biomedicine, ecology, optoelectronics, *etc.* Chemical and physical methods for the reduction of GO to obtain graphene-like materials similar in structure and properties to pure graphene obtained by direct mechanical cleavage are considered. Functionalization strategies of graphene materials are discussed. The preparation of hydro- and organogels as well as Pickering emulsions from graphene derivatives as precursors of porous monoliths are considered. The formation of aerogels based on graphene materials and methane adsorption on these porous structures are discussed. Basic information about hybrid materials containing graphene derivatives and metal-organic frameworks is given and their adsorption characteristics with respect to methane are evaluated. Covalent and noncovalent interactions in graphene – porphyrin hybrids are considered from the standpoint of formation of porphyrin architectures on the surface of graphene materials. Examples of the use of porphyrin – graphene composite materials in photo- and electrocatalysis, fuel cells and gas separation membranes are given.
The bibliography includes 243 references.

Contents

1. Introduction 776
2. Graphene as representative of 2D layered materials 777
3. Graphene oxide, a functionalized analogue of graphene 779
4. Preparation of graphene oxide. The Hummers method and its modifications 780
5. Reduction of graphene oxide 780
6. Chemical modification of graphene 781
7. Chemical modification of graphene oxide 782
8. Aqueous and organic dispersions of graphene oxide and reduced graphene oxide 782
9. Formation of graphene oxide and reduced graphene oxide gels 783
10. Pickering emulsions as precursors for homogeneous porous structures 784
11. Formation of monolithic aerogels based on graphene derivatives 785
12. Graphene materials as methane sorbents 787
13. Methane adsorption on hybrid materials containing graphene derivatives and metal-organic frameworks 789
14. Formation of porphyrin architectures on the surface of graphene materials. Covalent and noncovalent interactions in graphene – porphyrin hybrids 790
15. Composite materials based on porphyrins and graphene derivatives 793
16. Conclusion 794

Received 22 February 2019

© 2019 Uspekhi Khimii, Russian Academy of Sciences and Turpion Ltd.

1. Introduction

A considerable body of literature on graphene (a nearly 100-fold increase in the number of yearly published articles since 2004 [1]) characterizes both scientific interest in this novel 2D material and a great potential of its practical applications. It is expected that in the near future, graphene and other 2D materials will be used in various fields from electronics to gas storage and separation, catalysis, high-performance sensors, support membranes and inert coatings.[2]

Graphene, a single layer of graphite, has been one of the first real 2D materials. In the last five to ten years, considerable efforts were made to obtain single layers of graphite (graphene sheets). A particular goal of this research activity was to verify theoretical ideas about the possibility for this carbon material to exist and to determine its properties.

Most studies on separation of graphite layers were carried out before the mid-1990s. Their authors mainly focused on graphite intercalation compounds. In these systems (inclusion compounds), guest atoms, ions or molecules are sandwiched between graphite layers. An important role in the formation of such layered complexes is played by charge transfer from the guest subsystem to the host one or *vice versa*. Using amphoteric properties of the graphite matrix and partial charge transfer, dozens of graphite intercalation compounds were prepared. They have regular layered structures, exhibit high anisotropy of properties and allow one to vary the composition of the intercalated layer.

The precursor material for graphene is thermally expanded graphite (or exfoliated graphite) obtained by rapid heating of intercalated graphite followed by transition of the substance sandwiched between the graphite layers to the vapour phase. Porous sorbent thus formed possesses unique properties, *e.g.*, specific surface area of up to 200 $m^2\ g^{-1}$, bulk density of up to 0.8 $kg\ m^{-3}$ and the volume expansion factor up to a value of 1000.[3,4] Additional microwave treatment of intercalated crystalline graphite in the course of thermal expansion enables preparation of free graphene films a few atomic layers thick.[5]

Not only thermal expansion, but other methods were also used for graphite exfoliation before the 2000s; however, all of them gave graphene flakes a few layers thick.

Eventually, in 2004 researchers from A.Geim's group at Manchester University succeeded in isolating macroscopic graphene flakes one atom thick.[6] Although being simple, their method (scotch tape technique) cannot be used to form coatings on large-area substrates or to obtain large monoliths since the yield of single layers of graphite is low. However, extensive research carried out using the thermal expansion technique made it possible to solve various problems related to low-dimensional systems and, in particular, to prove that high-crystal-quality 2D materials can be stable under ambient conditions and are continuous on a macroscopic scale.

The results obtained, in particular, determination of unique mechanical, electrical, optical and other properties of graphene gave a strong impetus to the development of other (including cheap) methods for preparation of graphene sheets for subsequent assembly of graphene materials.

The most widely used methods for the synthesis of graphene sheets include chemical vapour deposition involving deposition of hydrocarbons on the surface of metals (Ir, Ru and Pt) and metal carbides, *in vacuo* thermal decomposition (graphitization) of SiC, organic synthesis, chemical method using colloidal dispersions based on compounds containing graphene sheets. At present, considerable efforts are made, aimed at developing readily scalable and economically viable technologies based on graphene solutions (dispersions). In this case, considerable attention is paid to

V.V.Arslanov. Doctor of Sciences (Chemistry), Professor, Head of Laboratory of Physical Chemistry of Supramolecular Systems at the IPCE RAS.
Telephone: +7(495)955–4489, e-mail: vladimir.arslanov@gmail.com
Current research interests: molecular and supramolecular design, planar ensembles with controlled structure, self-assembled molecular layers; hybrid nanostructured systems for nanoelectronics, noninear optics, bio- and chemosensorics; complexation of macrocyclic ligands with metal cations, adhesion and diffusion in polymeric systems.
M.A.Kalinina. Doctor of Sciences (Chemistry), Professor RAS, Leading Researcher of the same Laboratory.
Telephone: +7(495)955–4680, e-mail: kalinina@phyche.ac.ru
Current research interests: surface phenomena, self-assembly of colloidal systems, functional nanomaterials, hybrid materials, supramolecular systems, thin films, chemical sensors, heterogeneous catalysis.
E.V.Ermakova. Researcher at the same Laboratory.
Telephone: +7(495)955–4423, e-mail: evermakova92@gmail.com
Current research interests: supramolecular systems, Langmuir monolayers, Langmuir–Blodgett (Langmuir–Schaefer) films, chromoionophores based on anthraquinones and porphyrins, recognition, photoshromism, sensors, graphene oxide, bilayer porphyrin–graphene templates.
O.A.Raitman. Candidate of Sciences (Chemistry), Senior Researcher of the same Laboratory.
Telephone: +7(495)955–4423, e-mail: rightman@mail.ru
Current research interests: supramolecular chemistry, surface plasmon resonance, sensors, transducers, Langmuir–Blodgett monolayers and films, photochemistry.
Yu.G.Gorbunova. Corresponding Member of the RAS, Doctor of Sciences (Chemistry), Professor, Principal Researcher of IGIC RAS.
Telephone: +7(495)955–4874, e-mail: yulia@igic.ras.ru
Current research interests: coordination and supramolecular chemistry.
O.E.Aksyutin. Corresponding Member of the RAS and International Academy of Technological Sciences, Doctor of Engineering, Head of the Gas Transportation, Underground Storage and Utilization Department at Gazprom JSC.
E-mail: O.Aksutin@adm.gazprom.ru
Current research interests: hybrid materials, sorbents, gas separation.
A.G.Ishkov. Doctor of Sciences (Chemistry), Professor, Deputy Head of the same Department, Head of Energy Saving and Ecology Department at Gazprom JSC.
E-mail: A.Ishkov@adm.gazprom.ru
Current research interests: hybrid materials, sorbents, gas separation.
V.A.Grachev. Corresponding Member of the RAS, Doctor of Engineering, Professor, Principal Researcher at the Laboratory of Highly Concentrated Disperse System at the IPCE RAS.
Current research interests: carbon nanomaterials and composites, hybrid materials.
Telephone: +7(495)955–4642
A.Yu.Tsivadze. Academician of the RAS, Doctor of Sciences (Chemistry), Professor, Scientific Director and Head of Laboratory of New Physicochemical Problems at the IPCE RAS.
Telephone: +7(495)952–0462, e-mail: tsiv@phyche.ac.ru
Current research interests: chemistry of coordination compounds, chemistry of novel inorganic functional materials, supramolecular chemistry, radiochemistry.

Translation: A.M.Raevskiy

solution of the problem of low solubility of graphite. A promising approach involves transformation of graphite oxide used as the starting material into graphene oxide (GO), which is water-soluble when the particle size and oxidation level are chosen appropriately. This simple technique allows one to prepare solutions with sufficiently high concentrations of single-layer GO flakes.

In contrast to graphene, violation of aromaticity makes GO good insulator. Since many applications require conductive GO, the conductivity of the material can be recovered using chemical and physical methods. Optically transparent and conductive thin films of chemically reduced GO are thought to be candidates for replacement of metal oxides in electrodes for solar cells, while aqueous dispersions can be used as precursors for monoliths (hydrogels, Pickering emulsions, aerogels).

At present, fabrication of graphene monoliths with well-defined and controllable microstructure attracts considerable attention. This first of all concerns porous materials that can be used as gas (in particular, methane) sorbents.

Adsorption studies using porous graphene monoliths and especially activated graphene structures fabricated using reduction of GO demonstrated high methane, carbon dioxide and hydrogen adsorption capacity. There has been intensive research into hybrid materials based on porous graphene structures and metal-organic frameworks (MOF). However, application of MOF as methane storage units receives much more attention compared to hybrid systems.

The synthesis of hybrid structures based on graphene materials and porphyrins is based on the fundamental concepts of the interaction both between the aromatic platforms of components and between functional substituents grafted to the porphyrin ring and carbon substrate. Self-assembly of such functionalized porphyrin derivatives into ordered porous surface structures (MOF) occurs through metal – organic ligand coordination. These interactions allow one to obtain extended surface-bound supramolecular framework structures. Compared to other GO-based carbon materials, hybrid materials exhibit much higher catalytic activity, being competitive with the best commercially available Pt/C catalysts.

In this review the emphasis is placed on the preparation of hybrid materials using chemical liquid-phase approaches ('soft' chemistry methods) that provide the possibility of large-scale production and relatively simple and available methods for modification of the structure and properties of the materials being prepared depending on the field of application.

Notations are as follows:

a-3D-G — three-dimensional graphene material,

a-GDC — graphene derived carbon,

a-GODC — graphene oxide derived carbon,

ARPA-E — the US Advanced Research Projects Agency-Energy,

BET — Brunauer – Emmett – Teller,

Ce(TPP-Fc)(C22OPP) [TPP-Fc — 5-(4-(4-(ferrocenylphenylethynyl)phenyl)-10,15,20-triphenylporphyrin, C22OPP — 5,10,15,20-tetrakis(4-docosyloxyphenyl)porphyrin],

Cu-tbo-MOF — metal-organic framework with highly aromatic rigid octacarboxylate linker (tbo),

CVD — chemical vapour deposition,

DOE — the US Department of Energy,

EG — expanded graphite,

GO — graphene oxide,

mGO — modified graphene oxide,

rGO — reduced graphene oxide,

HKUST-1 — a Hong Kong University of Science and Technology material; MOF based on Cu^{2+} and benzene-1,3,5-tricarboxylic acid,

MIL-101 — a Materials Institute Lavoisier material; MOF based on benzene-1,4-dicarboxylic acid and chromium(III) cations,

MOF — metal-organic frameworks,

NT — nanotubes,

SEM — scanning electron microscopy,

SGH — self-assembled graphene hydrogel,

SSA — specific surface area,

STP — standard temperature (0 °C) and pressure (1 bar),

THPP — 5,10,15,20-tetrahydroxyphenylporphyrin.

2. Graphene as representative of 2D layered materials

Since the discovery [6] in 2004, graphene has justly held the rising star status [7] owing to unique properties (theoretically large surface area, high mechanical strength, optical transparency, thermal conductivity and high electron mobility). These unique properties of graphene, characteristic of nanometre scale, underlie intensive research into planar systems immediately after communications by Novoselov and Geim,[8] who were awarded the 2010 Nobel Prize in physics for the discovery of graphene.

High mechanical strength of graphene is of great importance for the preparation of monolithic architectures (aerogels, composites, *etc.*). Theoretically, a one-atom-thick graphene sheet measuring 1 m^2 can hold a mass of 4 kg (Fig. 1).

Owing to the 2D structure graphene is a highly flexible material which can be used for, *e.g.*, weaving (a graphene string will be as strong as a heavy steel cord). Besides, 'smart' graphene can exhibit the properties of a self-healing material under particular conditions. Graphene films are excellent water filters since they pass water molecules and hold all other molecules. Probably, in the future this will help to reduce the cost of seawater desalination. Researchers at Lockheed Martin Corp. (USA) developed a graphene water filter called Perforene, which reduces the energy expenditure for desalination by 99%.

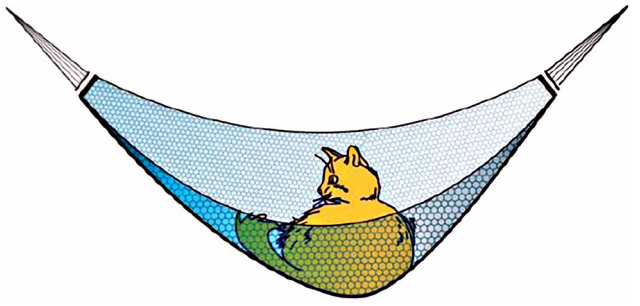


Figure 1. Mechanical strength of graphene: an illustration.[8] A hypothetical graphene hammock measuring 1 m^2 and weighting less than 1 mg can hold a 4-kg cat (*cf.* only 40 g for a steel hammock of the same surface area and thickness).

To date, main methods for the preparation of graphene include mechanical cleavage of graphene sheets from highly oriented pyrolytic graphite (HOPG); growth on substrates (chemical vapour deposition involving deposition of hydrocarbons on the surface of metals and metal carbides); organic synthesis; and a chemical method using colloidal dispersions based on graphene-containing compounds. Each method has its own advantages and disadvantages. For instance, mechanical cleavage (scotch tape technique) allows one to obtain best-quality samples; however, the method is labour-consuming and thus inappropriate to obtain graphene on a large scale. From the standpoint of commercial manufacture, it is chemical methods of synthesis that seem to be the most promising. Indeed, they are used to prepare colloidal graphene dispersions representing convenient systems for various technological applications. In the pioneering studies that gave rise to the 'graphene rush'[6] single graphene sheets were prepared by the so-called micromechanical cleavage, or the 'scotch tape technique', *viz*., a HOPG crystal was sandwiched between the scotch tape, which was then torn, holding microscopic graphite platelets. These platelets were again sandwiched between new scotch tape and the procedure was repeated. It was found that graphene flakes become visible under an optical microscope when placed on a silica substrate of a particular thickness (300 nm). This leads to an interference effect that allows one to unambiguously distinguish between the substrate and the single-layer structure. For instance, if the substrate is only 5% thicker (315 nm *vs*. 300 nm), graphene crystallites placed on the substrate become completely invisible.[9] Using various narrow-band filters, clear images of graphene flakes on substrates of different thickness can be obtained.[10]

A practically important line of investigations is the preparation of graphene from expanded graphite (EG), which is also called thermally expanded graphite. It is formed upon rapid heating of graphite intercalation compounds. When they are heated in the heat shock mode, the pressure of the intercalate in the interplanar space abruptly increases, which leads to exfoliation of the graphite scaffold and the formation of a porous defective carbon structure composed of layered graphite domains. Expanded graphite is obtained from graphite bisulfate or graphite nitrate. Usually, EG represents multilayer graphene stacks 30 – 100 nm thick, which corresponds to hundreds of graphene sheets. Attempts to subsequently foliate EG under prolonged sonication in alcohol were unsuccessful since the stacks remained more than 50 nm thick.[11] Combining alcoholic and acidic treatment led to better results, *viz*., graphene flakes 6 – 7 nm thick were obtained. Graphene colloids can be prepared using both EG of industrial origin and new forms of EG containing only 10 – 15 graphene sheets.[12]

Graphene can also be obtained from graphite using chemical methods. One of them involves treatment of graphite with a mixture of sulfuric and hydrochloric acids. Oxidation leads to the appearance of carboxyl groups at the edges of the sample. Then, carboxyl groups are transformed to chlorides upon treatment with thionyl chloride. Subsequently, graphene layers are formed under the action of octadecylamine in tetrahydrofuran, tetrachloromethane or dichloroethane.[13]

Chemical vapour-phase deposition (CVD) is an efficient method for the growth of large-area graphene films.[14] The key stages of the method include deposition of a graphene layer on a copper substrate followed by transfer of this layer to a dielectric substrate. Almost any organic material can be used as the source of carbon for the deposition on metallic substrates. For instance, Tour and co-workers[15] prepared high-quality graphene on a copper substrate from food, waste and even insects. However, CVD is expensive due to large energy consumption and the need to remove the metallic (copper) layer.[14]

Other methods for the preparation of graphene include the synthesis of polyphenylenes followed by cyclodehydrogenation,[16] radiofrequency plasma-enhanced chemical vapour deposition[17] and high-pressure – high-temperature growth process.[18] However, it seems unlikely that they will become economically viable in the next decade.

The properties and, therefore, the potential of practical application of graphene depend strongly on the quality of the material and substrate, on the type of defects, *etc*. (Table 1).[19]

Table 1. Properties of graphene prepared by different methods.[19]

Method	Crystallite size /μm	Sample size /mm	Charge carrier mobility at 293 K /cm^2 (V s)$^{-1}$	Application field
Mechanical exfoliation	> 1000	> 1	$> 2 \times 10^5$ and $> 2 \times 10^6$ (at low temperature)	Research
Chemical exfoliation	⩽ 0.1	∞ for a layer of overlapping flakes	100 (for a layer of overlapping flakes)	Coatings, paints, ink, composites, transparent conductive layers, *etc*.
Chemical exfoliation *via* graphene oxide	~ 100	∞ for a layer of overlapping flakes	1 (for a layer of overlapping flakes)	Coatings, paints, ink, composites, transparent conductive layers, *etc*.
Chemical vapour deposition	1000	~ 1000	10 000	Photonics, nanoelectronics, transparent conductive layers, sensors
In vacuo SiC graphitization	50	100	10 000	High-frequency transistors, various electronic devices

Since the discovery of graphene, hypothetical graphene-based devices utilized unique physical properties of this 2D material (touch screens, solar cells, energy storage units, cell phones, ultrafast chips). Recently, the prospects of graphene as alternative to silicon as the basic unit of the electronics industry have been discussed.[20, 21]

At present, studies on the synthesis and properties of graphene represent one of the most widely discussed and rapidly developing field in chemistry and physics. Of particular interest is the possibility to fabricate unique monolithic hybrid porous structures based on graphene and its derivatives.[22–24]

Concluding this Section, mention may be made of the advantages and drawbacks of the main method for the preparation of graphene.

To date, best-quality graphene samples are obtained using the scotch tape technique; the method is labour-consuming and gives a low yield of the product. Clearly, it is inappropriate for large-scale production of graphene, being on-demand for basic and applied research into many properties of the material. As to the growth of graphene on substrates, the crucial point is to control the growth of a single layer of graphene and to exclude the growth of subsequent layers. Next, large polycyclic aromatic molecules can be treated as graphene nanosheets. However, they are difficult to synthesize since the solubility of polycyclic aromatic compounds decreases appreciably with increasing number of fused rings and owing to the occurrence of side reactions.

The advantages of liquid-phase chemical approaches ('wet' or 'soft' chemistry methods) to the synthesis of graphene are as follows: they are suitable for large-scale production of graphene and allow one to modify the properties of the material with relative ease depending on the field of application. Note also that conversion of graphene into colloidal dispersions is necessary to perform certain processing steps (impregnation, mixing, deposition, functionalization) and for various applications (hydrogels and aerogels, Pickering emulsions, adsorbents, membranes, *etc.*).

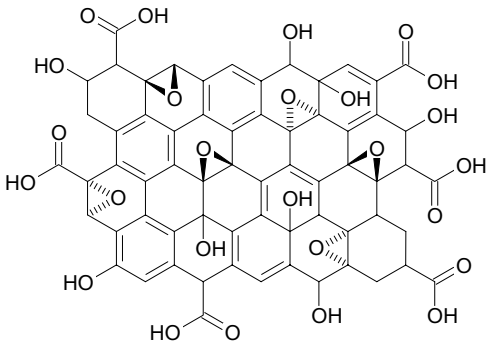
3. Graphene oxide, a functionalized analogue of graphene

Graphite oxide, a material related to GO and often treated as an analogue to GO, was for the first time synthesized more than 150 years ago.[25] The synthesis was based on the oxidation of graphite. Since then the chemical strategy for preparation of colloidal dispersions of graphite has remained essentially unchanged, although some modifications were proposed. The C : O ratio for graphite oxide is in the range of 1.62–2.57. For GO, the C : O ratio varies from 2 to 4 and corresponds to the chemical compositions ranging from $C_8O_4H_5$ to $C_8O_2H_3$.[26]

Graphite oxide (Fig. 2) has a multilayer structure in contrast to mono- or few-layer GO. This is the main difference between the two materials. The C : O and C : H ratios depend on the starting material and on the character of the oxidation process (chemical composition and relative amount of the oxidizing agent, the temperature and duration of the process, the presence and character of the activation factor). An interesting optical property of GO is intrinsic fluorescence in near-IR, visible and UV regions. This feature distinguishes GO from graphene; the latter is a zero-band-gap semiconductor and exhibits no fluorescence.

Among graphene derivatives, the most attention is paid to GO, reduced (most often, partially) graphene oxide (rGO), graphite and graphite oxide. Graphene oxide is a complex chemical system composed of graphene nanosheets (nanoleaves, nanoflakes) decorated with covalently bound oxygen-containing groups. Epoxy and hydroxyl groups are arranged on the basal plane, while carbonyl, carboxyl and lactone groups decorate the edges of GO nanosheets.[28] Although GO is made of only three chemical elements (C, O and H), there is a variety of oxygen-containing functional groups bound to different regions of nanosheets constituting the material. The chemical composition of GO was thoroughly analyzed by IR spectroscopy.[29] The structure of graphene flakes bearing typical functional groups was also considered elsewhere.[30]

The structure of graphene oxide



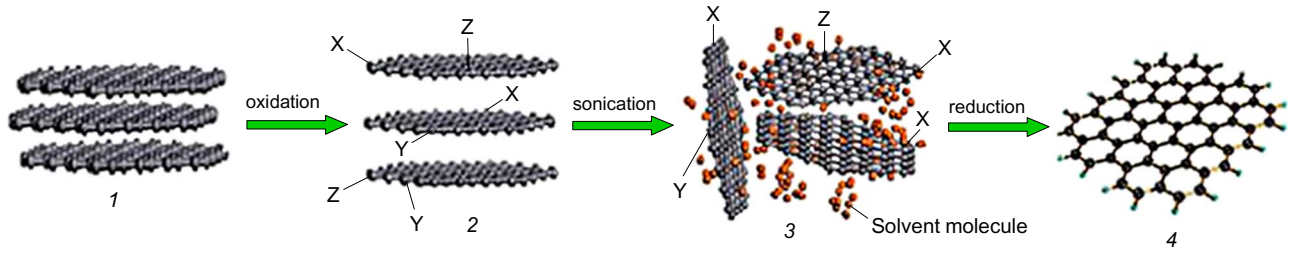


Figure 2. Preparation of graphene *via* intermediate formation of graphene oxide.[27]
Natural graphite (*1*) as starting material; graphite oxide with oxygen-containing groups X, Y and Z (*2*); graphene oxide obtained upon sonication of graphite oxide and comprising both single-layer and multilayer graphene sheets (*3*); and reduced graphene (number of layers in graphene sheets depends on the method of preparation; residual oxygen-containing groups X, Y and Z are also present) (*4*).

4. Preparation of graphene oxide. The Hummers method and its modifications

There is a number of methods for preparation of GO by the oxidation of graphite.[31,32] The highest and lowest content of oxygen in GO and graphite oxide is attained using the Staudenmaier (C : O = 2.9 : 1.0) and Brodie methods, respectively.[33] However, it should be noted that the C : O ratio depends not only on the method, but also on the duration of the oxidation process. The average size of GO flakes can be controlled by varying the oxidation conditions.[34] The oxidation is accompanied by an increase in the interplanar spacing of graphite from 0.34 to ~0.6–1.2 nm depending on the extent of oxidation.[35] The large van der Waals gap allows water molecules to exist in the interplanar space;[36] this to some extent influences the aqueous dispersibility of GO. The yield of GO also depends on the size of the starting graphite crystallites.[37] Microcrystalline graphite has a defective structure, its oxidation affords GO in low yield, as well as CO_2 and CO. The oxidation of macrocrystalline graphite results in much higher yield of GO (up to 95%).

In the vast majority of cases, GO is obtained by the Hummers method and its modifications. The method uses a strong mineral acid and $KMnO_4$ as oxidizing agent.[38] The classical procedure assumes the use of graphite (100 g), concentrated H_2SO_4 (2.3 litre), $NaNO_3$ (50 g) and $KMnO_4$ (300 g). Potassium permanganate is slowly added to a mixture of other reactants cooled to 0 °C and the temperature of the reaction mixture is maintained below 20 °C. After the reaction mixture is kept at 35 °C for 30 min, water (4.6 litre) is added and the temperature rises to 98 °C. After 15 min, the reaction mixture is diluted in water and then treated with H_2O_2 to reduce Mn^{VII}, and the residue formed is filtered off. To remove residual cations and anions, the residue is again dispersed in water and treated with cation and anion exchangers. The C : O atomic ratio in the product is 2.3 : 1.0. The technique using H_2SO_4 leads to replacement of GO by some amount of sulfonic groups along with other functional groups.[39] The classical method by Hummers and Offeman gives a product with a specific surface area in the range of 40–50 $m^2\ g^{-1}$. A modification of the Hummers method was reported.[40] To concentrated H_2SO_4 (98%, 70 ml), a natural graphite powder (1.5 g) and $NaNO_3$ (1.5 g) are added in an ice bath and then $KMnO_4$ (9 g) is added slowly at 10 °C. The mixture is heated to 30 °C and kept at this temperature for 10 h. Then deionized water (100 ml) is added dropwise and the mixture is kept at 90 °C for 2 h. The suspension thus obtained is diluted with water and 30% H_2O_2 (30 ml) is added. The mixture is centrifuged and washed with HCl until pH 7. In the final step, water is removed at reduced pressure and 50 °C.

Modified Hummers methods were used by different authors.[41–45]

It was found that no deep oxidation of graphite is needed to obtain single-layer GO.[46]

Interesting chemical transformations of oxygen-containing groups and slow equilibration of their chemical compositions in GO were reported.[47] Namely, after 35 days since the oxidation using the Hummers method the concentration of epoxy groups decreased while that of hydroxyl groups increased. The contents of these groups equilibrated only after storage of the GO sample at room temperature for three months.

In his attempts to determine the molecular mass of graphite Brodie[48] oxidized the material using strong acids (HNO_3, H_2SO_4) and $KClO_3$. Emphasize that this approach involves the evolution of gaseous ClO_2 and is fraught with danger of explosion. The specific surface area of the product is 2 $m^2\ g^{-1}$.

The Staudenmaier method[49] is the development of Brodie's technique, It involves the addition of $KClO_3$ to a dispersion of graphite in a mixture of concentrated HNO_3 and H_2SO_4 (1 : 2 v/v).

There are also modified versions of the methods described above, which involve variation of oxidants and their ratio, as well as the oxidation and product isolation conditions.

5. Reduction of graphene oxide

Unlike highly conductive graphene, GO exhibits the properties of a dielectric, thus being deprived of attractive prospects offered for the former material.

Therefore, there has been intensive research into reduction of GO in order to significantly increase its conductivity.

The most obvious goal of the reduction is to prepare graphene-like materials that are similar in structure and properties to pure graphene obtained by mechanical cleavage of single layers of graphite (scotch tape method). In spite of numerous research efforts, this goal is not yet achieved. Residual functional groups and defects fundamentally change the structure of the carbon sheet and therefore rGO should not be identified as graphene since their properties are significantly different. The properties of rGO depend on the method of reduction, which in turn influences the final characteristics of materials containing or devices based on rGO. Although graphene with perfect structure was not prepared as yet *via* the reduction of GO, researchers continuously improve the structure of the final product in a desired direction.

The most widely used reducing agents are aqueous hydrazine solutions or anhydrous hydrazine; however, dimethylhydrazine, hydroquinone and other compounds are also used.

As reduction of GO dispersion develops, the hydrophilicity of GO gradually decreases, and the reduced graphene sheets precipitate. The residue cannot be redispersed even under sonication or under the action of surfactants.[50] To preclude irreversible aggregation, various stabilizers are introduced into the reaction medium. These are polymers, surfactants, biomolecules or large aromatic donor or acceptor molecules that can stabilize graphene nanosheets through π–π interactions. Other methods for stabilization of rGO colloids involve the use of bifunctional reactants that simultaneously act as reducing agents and stabilizers or solvents and thorough control of the reduction conditions. Graphene dispersions are also stabilized using covalent modification of graphenes.[26]

Treatment of GO with concentrated alkali on heating to moderate temperatures (50–90 °C) leads to removal of oxygen-containing groups without participation of other reducing agents.[51] Dispersions thus prepared are stable on the time scale of a few days since in alkali medium one deals with deprotonation of residual carboxyl groups, which ensures electrostatic repulsion between rGO nanosheets. The reaction rate depends on the medium pH, *viz.*, the higher the pH value the faster the reduction. Besides,

reduction of GO can proceed under specific conditions, *e.g.*, under the action of hydrazine (supercritical conditions)[52] or immediately under the action of organic solvents or water.[53]

In addition to the reduction of GO to rGO using chemical agents under conventional or specific conditions, thermal[54, 55] and microwave-assisted solid-phase reduction of GO[56] are used.

The reduction of GO is needed for many applications of the material.[26, 50] The main goal of the reduction process is to remove oxygen-containing functional groups (epoxy, hydroxyl, ketone and carboxyl ones).

Heat treatment is an efficient and very simple method for the reduction of GO, which significantly decreases the content of oxygen-containing groups in GO. The process is accompanied by considerable mass loss and distortion of the crystal structure of GO owing to desorption of structure-forming components from the surface and from the bulk of the material. From the standpoint of large-scale production, low-temperature reduction at temperatures below 450 °C is of great importance since it leads to efficient modification of the properties of GO and induces only slight structural distortions.[57] The influence of reduction on the physicochemical properties of GO in the temperature range from 200 to 400 °C was studied.[58] Using Raman spectroscopy, it was shown that low-temperature reduction in argon atmosphere causes a decrease in the intensity of the D peak relative to the G peak and a shift of position of the maximum of the G peak towards lower frequencies. It was found that thermal reduction leads to a decrease in the intensity of the IR absorption lines corresponding to hydroxyl groups. Removal of oxygen-containing functional groups is accompanied by significant decrease in the electrical resistance from values exceeding hundreds of MΩ to 20 kΩ. A surface morphology study by electron microscopy and atomic force microscopy revealed no destructive influence of heat treatment on the crystal structure of GO.

Microwave-assisted mild thermal reduction of GO was also reported.[59] The reduction of GO can be accomplished within a few minutes in high yield while the extent of reduction depends on the duration of microwave treatment at a given power (800 W).

Interestingly, the electrical conductivity of the rGO paper is nearly 10^4 times higher than that of GO paper.[59]

Electrochemical reduction is an environmentally safe method that allows one to rapidly obtain high-purity rGO.[60]

Tkachev[61] described a method for the preparation of gram amounts of graphene by reduction of GO by supercritical isopropyl alcohol. Methods for preparation of GO and graphene in various solvents were proposed. The action mechanism of high-power ultrasound on the starting graphite – water – surfactant with the formation of nanographite dispersion was substantiated. Based on the known ideas about the interaction of high-power ultrasound with matter, Tkachev proposed that cavitation bubbles that appeared during the treatment process penetrate into the intercrystalline or interlayer space of the graphite structure. Collapse of cavitation bubbles is accompanied by the onset of secondary shock waves that initiate bond dissociation in and structure breakdown of graphite (Fig. 3).

6. Chemical modification of graphene

Improvement of methods for the preparation of graphene, GO and rGO is accompanied by intensive search for procedures of chemical modification of these nanosystems in order to develop methods for controlling (i) the reactivity of the graphene surface including peripheral regions and (ii) the electronic and other properties to design novel materials and devices.[62]

Graphene is characterized by relatively low chemical activity; its electronic structure is such that π-electrons are completely delocalized over the entire 2D network. There-

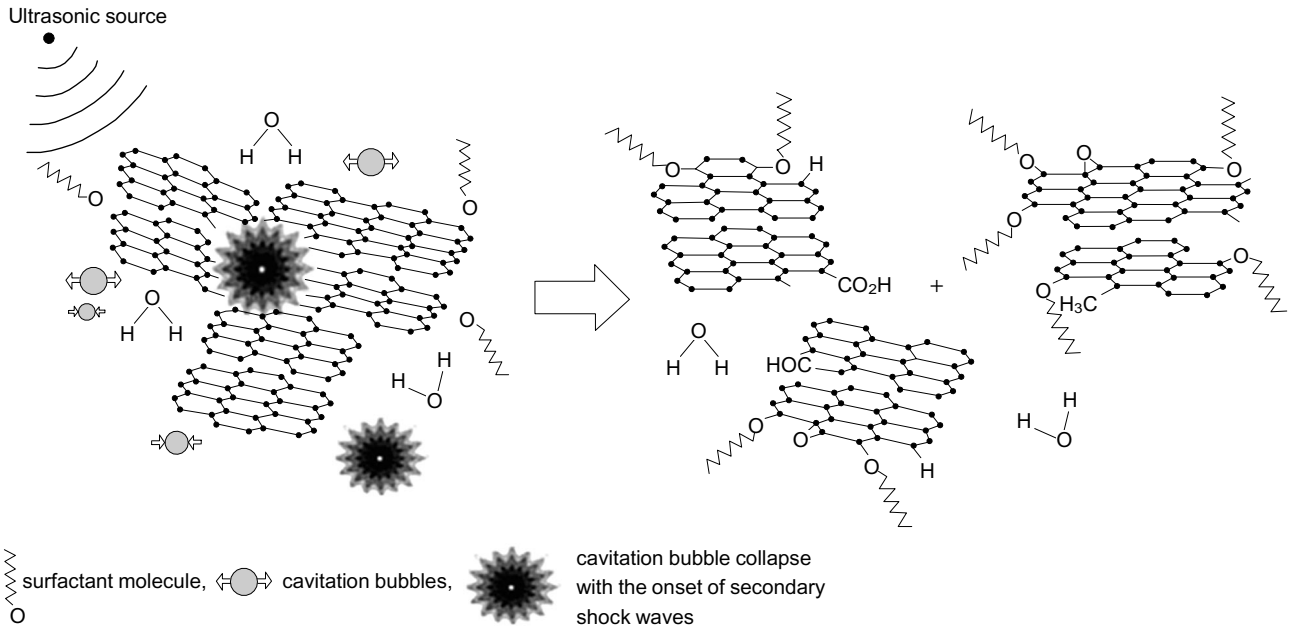


Figure 3. Interaction of cavitation bubbles with graphite layers resulting in nanographite.[61]

fore, chemical modification of graphene is only possible using rather highly reactive reactants.

It should be noted that no exact data on the dependence of the reactivity of graphene nanosheets on their size and shape, and on the possibility of controlling the stoichiometry are available at present. The formation of a covalent bond on the basal plane of a graphene sheet causes the appearance of sp^3-hybridized carbon atoms. The reactivity of adjacent surface domain increases, thus inducing a 'chain' reaction starting from the primary attacked point. Strained regions also exhibit enhanced reactivity. Both types of graphene edges, zigzag and armchair ones, also have different reactivities since the zigzag structure is thermodynamically unstable and more reactive. Graphene sheets can participate in hydrogenation and fluorination reactions as well as in the addition of various functional groups and inorganic species. These reactions were considered in reasonable detail in a review [63] and in other publications.[53, 64 – 70]

It was established that single graphene sheets are ten times more reactive than graphene multilayers and that the reactivity of graphene edges is twice as high as that of the basal plane atoms.[71]

7. Chemical modification of graphene oxide

The surface of GO is decorated with numerous functional groups and can therefore be chemically modified using classical organic reactions that make it possible to finely tune the chemical and physical properties of the material. Methods used to solve this problem depend strongly on the field of application of the material being designed. In a broad sense one can consider functionalization of peripheral regions of GO nanosheets and functionalization of the basal plane. In the former case modification is achieved using the reactivity of carboxyl groups, while in the latter case modification is based on the reactivity of hydroxyl and epoxy groups bound to the basal plane.[31, 72]

Often, certain properties of functionalized GO derivatives are not typical of the starting GO. For instance, to make 'water-soluble' GO dispersible in organic solvents in order to prepare organosols or to attain compatibility with polymers, the surface hydrophilic groups of GO are converted to hydrophobic ones. The character and intensity of interphase interactions can be tuned with high accuracy. Hydrophobization of the surface decreases its water affinity, which resembles the behaviour of rGO.

Directional functionalization of GO allows one to assembly complex systems with various properties, *e.g.*, enhanced (or induced) hydrophilicity or hydrophobicity, as well as increased thermal stability and mechanical strength. Therefore, functionalized GO derivatives are used in polymeric composites, drug delivery systems, sensors and electrochemical devices.[73] Among various aspects of functionalization of GO, control of chemo- and regioselectivity is still to be clarified. For instance, when carrying out amidation of carboxyl groups of GO under the action of $SOCl_2$ or carbodiimide coupling, the exogenous amine can simultaneously functionalize the basal plane *via* ring-opening of the epoxy group. Therefore, modification of functional groups of GO can occur in different regions of GO nanosheets depending on the reaction conditions. The modification of GO thus remain an important tool in the design of novel materials.

8. Aqueous and organic dispersions of graphene oxide and reduced graphene oxide

In addition to research into graphene and its derivatives as 2D materials considerable efforts were made to design 3D structures that retain and utilize the properties of nanosheets on the macroscopic level and represent a novel type of materials. In this case, practical implementation of the advantages provided by graphene requires large-scale synthesis, *i.e.*, integration of individual graphene units into complex multifunctional (monolithic) structures. In most cases the 3D structures in question are formed using aqueous and organic dispersions of graphene and graphene derivatives.[74] It is expected that the 3D structures will exhibit the properties resulting from synergistic combination of the properties of graphene and the new 3D architecture of the ensemble. The first and foremost task in the design of practically useful 3D structures is to fabricate consistent, adaptable and predictable graphene architectures by varying the parameters of the assembly and to understand the interrelations between structural ordering and the properties of materials. These problems were topical over decades for metallic and ceramic foams.[75, 76] The influence of polarity of organic solvents on the properties of graphene dispersions was studied.[77, 78] It was reported that homogeneous dispersions of single-layer graphene nanosheets in organic solvents similar to aqueous GO dispersions cannot be prepared since hydrophobic graphene is prone to aggregation due to van der Waals interactions between adjacent sheets. Aggregation leads to a considerable decrease in the surface area and leads to significant decrease in adsorption of porous monoliths.

The leading role in the preparation of dispersions, *i.e.*, precursors for monoliths, is undoubtedly played by GO whose precursor is graphite oxide. As mentioned above, graphite oxide is a layered material comprised of oxidized graphene sheets and characterized by high hydrophilicity owing to high content of functional groups. The interplanar spacing in graphite oxide differs from that in graphite and lies in the range from 3.4 to 12 Å. Graphite oxide layers bear a negative charge, which enables the formation of aqueous suspensions.[79] A drawback of dispersions based on graphite oxide is that dispersed particles are composed of a large number of aggregated nanosheets.

Graphite oxide can form colloidal solutions not only in water, but also in alcohols and other polar solvents as well as separate into thin (up to single-layer) nanosheets upon appropriate treatment.[80, 81]

In aqueous dispersions, GO nanosheets are electrostatically stabilized by peripheral carboxyl groups.[82, 83] These groups are responsible for high aqueous dispersibility of GO and stabilize aqueous dispersions after chemical reduction of epoxy and hydroxyl groups [84] on the basal plane.[85] The aqueous dispersibility of GO nanoparticles can be additionally increased by oxidizing hydroxyl groups on the basal plane to carboxyl ones.[86] Taking into account the importance of these functional groups for stabilization of GO dispersions, it was assumed [87] that fragmentation of graphene nanosheets into smaller pieces bearing no carboxyl groups on the freshly formed edges should decrease the dispersibility of nanosheets, but not induce their irreversible aggregation (Fig. 4 *a*). To test this hypothesis, sonication was used as an efficient tool to reduce the size of GO nanosheets [88] in a dilute (2 mg ml^{-1}) aqueous

dispersion. Noteworthy, such dispersions gelate after 30 min of sonication (see Fig. 4 *b*).

The possibility to prepare aqueous GO dispersions ('solutions') is an important factor responsible for the formation and properties of various materials based on GO and rGO. The aggregative stability of dispersions first of all depends on the acidity of aqueous solutions and monotonically increases with increasing pH. Changes in 'solubility' are due to cleavage of hydrogen bonds between carboxyl groups of contacting nanosheets. The complex character of this dependence originates from different nanoparticle geometries and inhomogeneous distribution of carboxyl groups on their surface. A comparative experimental and molecular dynamics study of the pH-dependent behaviour of GO sols showed that at low pH, GO is protonated and forms aggregates.[89] At high pH, deprotonated carboxyl groups endow the GO nanosheets whith hydrophilic properties and the ability to form aqueous colloidal solutions. It was also established that dried single-layer GO nanosheets form dense aggregates with a complex structure and small specific surface area, as determined by the Brunauer – Emmett – Teller (BET) method.[90]

We believe that it is the simplicity and reliability of GO preparation by the Hummers method and its modified versions that are responsible for the popularity of GO among chemists working in the field of materials science and for increased interest in GO as versatile nanosized structural block in the synthesis of materials.

A study[91] of aqueous GO dispersions gave interesting results. Aqueous dispersions of GO nanosheets prepared by exfoliation of graphite oxide were treated with dye solutions (neutral red, brilliant green and rhodamine). It was found that the addition of dyes leads to failure of aqueous suspensions and precipitation of GO and that the residues separated from excess dye form stable suspensions of coloured GO nanosheets in water or *N*,*N*-dimethylformamide after re-dispersion. Colouration of GO nanoparticles is accompanied by a shift of the main absorption bands of the dyes towards longer wavelengths. Besides, the dye stability against UV irradiation increases significantly upon applying the dye to the GO nanosheets.

9. Formation of graphene oxide and reduced graphene oxide gels

Many studies are aimed to prepare homogeneous GO hydrogels and appropriately treat them using physicochemical methods in order to subsequently assemble 3D architectures (*e.g.*, aerogels).[7, 92, 93]

By definition, a gel is a colloidal system representing a suspension of liquid particles in a solid. The volume fraction of the solid component in the gel is much lower than that of the liquid component. The solid component has the form of nano- and microparticles brought into contact with one another and thus forming a branched network of chains and nanosheets that continuously penetrates the entire volume of the gel. That is why gels show no fluid behaviour, being jelly-like or even elastic rather than liquid. If the liquid phase is completely replaced by a gas (*e.g.*, air), an aerogel is formed.

Stable and homogeneous aqueous GO dispersions as precursors for monolithic 3D networks are often prepared using gel-forming molecules (*e.g.*, small organic molecules including amides, peptides, ureas, saccharides, nucleotides, molecules bearing long alkyl chains or steroid derivatives). After gelation these organic additives form chemical or physical cross-links that eventually stabilize the 3D structure and functional properties of the material prepared.

Since the assembly of GO-based structures offers certain advantages (water as medium, the possibility of dispersion to single-layer nanosheets and their chemical modification, relative simplicity of control of the assembly process), it is GO that is most widely used as precursor for monoliths. Monolithic graphene-based structures are formed using hydrothermal reduction, chemical reduction, as well as physical methods leading to formation of highly cross-linked graphene hydrogels.[94] The content of oxygen in the final product depends on the reduction conditions (*e.g.*,

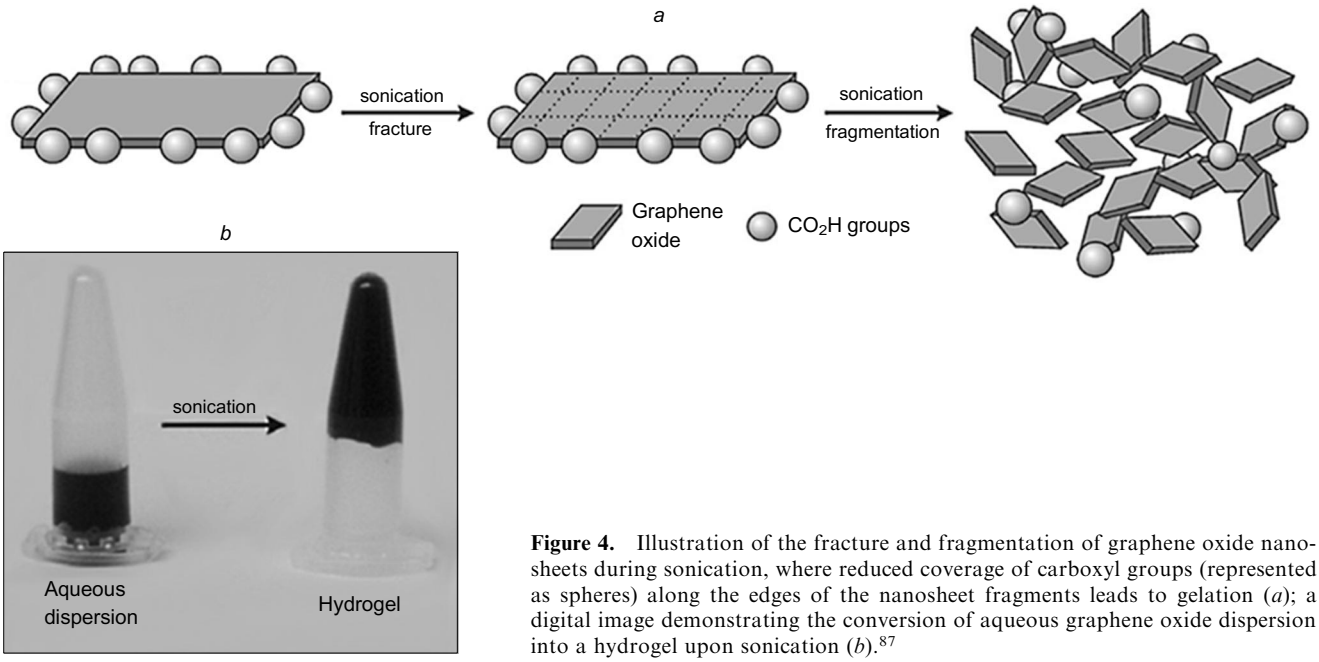


Figure 4. Illustration of the fracture and fragmentation of graphene oxide nanosheets during sonication, where reduced coverage of carboxyl groups (represented as spheres) along the edges of the nanosheet fragments leads to gelation (*a*); a digital image demonstrating the conversion of aqueous graphene oxide dispersion into a hydrogel upon sonication (*b*).[87]

temperature) and usually lies in the range of 10 at.% – 15 at.% except procedures involving post-thermal treatment. At temperatures above 900 °C, *i.e.*, at lower content of oxygen, one deals with the formation of mechanically strong and ultralight aerogel monoliths. Each method for reduction of GO (see above) has its own advantages and the choice of particular approach depends on the ultimate goal. The absorbed water is removed by freeze-drying or supercritical drying.[95]

In some cases, graphene nanosheets are assembled using no gel-forming agents. Namely, porous 3D GO materials (or even multilayer free films) are assembled from colloidal suspensions of untreated GO nanosheets (no additives) using joint action of vacuum evaporation, temperature and centrifugal force. Thermal annealing at 800 °C in H_2/Ar stream leads to formation of spongy rGO and rGO films containing less than 5 mass % of oxygen.[96]

Hydrogels based on rGO attract considerable attention due to unique architecture and useful properties. Compared to GO-based hydrogels, the former are characterized by higher mechanical strength and electrical conductivity as well as excellent thermal, chemical and electrochemical stability.[97, 98]

Main strategies for the preparation of hydrogels are shown in Fig. 5. Hydrogels based on GO offer certain advantages that are specified by the properties of GO nanosheets. These particles readily form hydrogels in water in the presence of various gel-forming agents. The hydrogels thus formed are composed of 2D GO domains decorated with oxygen-containing functional groups; they have large specific surface areas and can be controlled with ease using external factors. This lays the groundwork for various potential applications, such as adsorption, separation, sensorics, purification, drug delivery, *etc.*[99]

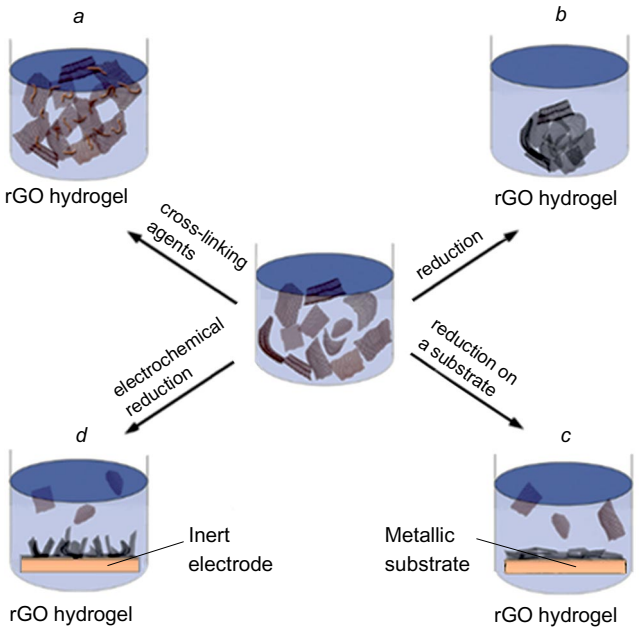


Figure 5. Schematic illustration of the main strategies of the preparation of graphene gels of different morphology.[99]
Graphene oxide hydrogels formed using gel-forming agents, low volume shrinkage (*a*); rGO hydrogels formed after chemical reduction of graphene oxide, high volume shrinkage (*b*); rGO hydrogels formed after chemical reduction of graphene oxide on a metallic substrate (*c*); and rGO hydrogels formed after electrochemical reduction of graphene oxide on an inert substrate (*d*).

The formation of GO hydrogels under sonication without using gel-forming agents was reported.[87] Sonication induced fracture of GO nanosheets into smaller fragments whose as-prepared edges were not decorated with functional (carboxyl) groups. Taking account of importance of these groups for stabilization of the dispersion, gelation in the absence of carboxyl groups was explained by changes in the chemical properties of the GO surface. Another situation was observed when GO was prepared from graphite powders of different size by the Hummers method. In this case smaller GO nanosheets are better 'dissolved' in water owing to higher specific concentration of carboxyl groups.[100, 101]

The formation of GO-based hydrogels using no additional solid templates requires considerable efforts to ensure the assembly of homogeneous architectures with specified cell size. A possible method for solving this problem is to prepare Pickering emulsions.

10. Pickering emulsions as precursors for homogeneous porous structures

Pickering emulsions are dispersions stabilized by solid particles immobilized at oil – water interface rather than conventional emulsifiers (surfactants). This type of emulsions was named after S.Pickering,[102] who described them in 1907, although the effect was discovered by W.Ramsden [103] in 1903. This type of emulsions was for long used only in food and cosmetics industries. In the last decades, Pickering emulsions have attracted considerable interest in connection with prospects for green and economic production of hybrid polymer particles and nanocomposites with supramolecular colloidal structures. Both emulsion or suspension polymerization in Pickering emulsions makes possible *in situ* preparation of reinforced nanostructured polymeric composites, unusual latexes and microcapsules with unique properties.

As we mentioned recently,[104] the ease of preparation of stable adsorption layers at the oil – water interface is due to the fact that adsorption of GO on the interface leads to better compensation of the GO surface domains of different energy compared to the case where air is the second phase. The effect is of particular importance for the formation of Pickering emulsions.

It is assumed that the ability of GO to exhibit the properties of adsorption-active substance to a great extent depends on the nature (polarity) of the oil phase, which was in fact ignored earlier. Graphene oxide-stabilized Pickering emulsions were studied in most detail by He *et al.*[105] They discussed the influence of various factors on the properties of Pickering emulsions and demonstrated the possibility to use these systems as catalysts for reduction of 4-nitrophenol to 4-aminophenol. The assembly of graphene monoliths were not considered.

Demulsification of oil (heavy petroleum) – water Pickering emulsions stabilized by GO and rGO nanosheets was studied [106] in connection with petroleum recovery problems.

Considerable attention is paid to the use of GO as stabilizer of emulsion polymerization of styrene, methacrylate, *etc.*[107 – 109]

The application of GO nanoparticles as seeds rather than stabilizers of seeded emulsion polymerization made it

possible to significantly improve the monodispersity of emulsions.[110]

A recent study[111] was carried out using GO modified with alkyl chains of different length (mGO). Grafting occurred as a result of the reaction between GO and alkylamine and led to reduction of GO. Compared to GO-stabilized oil-in-water emulsion, all mGO-stabilized emulsions were of the water-in-oil type. The mGO-stabilized emulsions demonstrated high stability in a wide range of pH and ionic strength values.

Perfect single-layer graphene is often treated as giant polyaromatic molecule having a large surface area, whose surface is accessible from both sides and which can undergo various reactions by analogy with unsaturated systems in organic molecules.[112] This feature of GO nanosheets allows one to modify them in order to improve various properties of the nanoparticles including the hydrophilic-lipophilic balance.

Thus, 2D nanoparticles such as GO nanosheets can stabilize Pickering emulsion owing to efficient adsorption at the oil–water interface. Studies on Pickering emulsions stabilized by GO or its derivatives (including rGO and mGO) are scarce. The same holds for investigations of the assembly of 3D monolithic architectures (aerogels) from Pickering emulsions and determination of factors responsible for the properties of the fabricated materials.

11. Formation of monolithic aerogels based on graphene derivatives

Aerogels are widely used to solve various scientific and applied problems since they have large surface area, low density and ultrathin pores.[113]

Usually, aerogels are prepared from hydrogels by supercritical drying. The advantage of this approach is that the structure of the initial gel is retained, whereas in the case of conventional drying the subsiding liquid shrinks and breaks up the network formed by nanoparticles. There is no liquid/gas phase boundary in a supercritical fluid, and, consequently, there is no surface tension.

Vacuum freeze-drying is yet another method for drying gels with retention of their structure. Since in this case water is removed through sublimation of the dispersion medium, the process can proceed only *in vacuo*. Correspondingly,

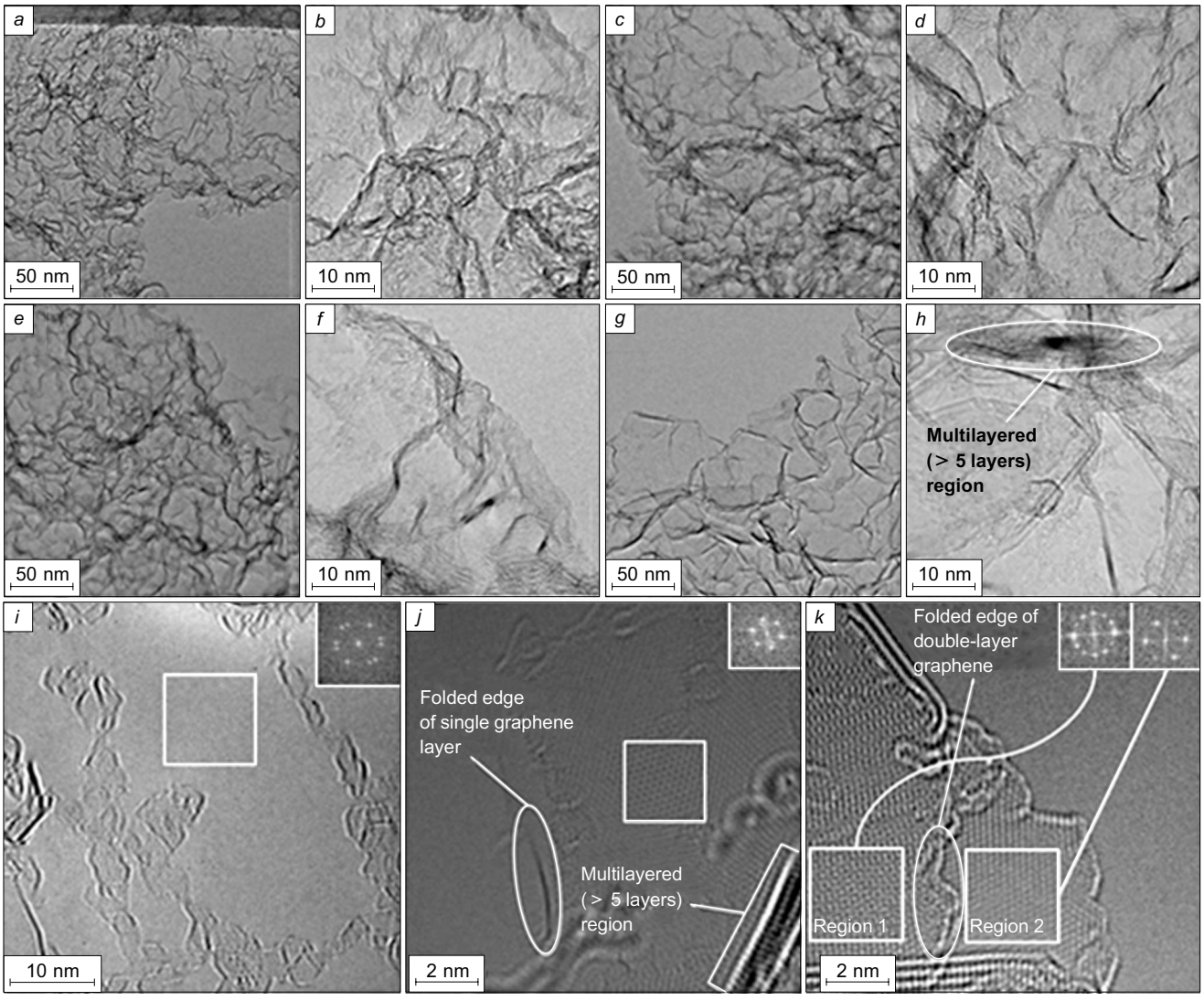


Figure 6. HRTEM images of graphene oxide aerogel annealed at 1050 (*a*, *b*), 1500 (*c*, *d*), 2000 (*e*–*g*) and 2500 °C (*h*–*k*).[94]

capillary forces have no effect on the gel structure under vacuum freeze-drying and supercritical drying conditions.

The structure of aerogels predetermines their unique properties. Although the strength of aerogels can approach that of solids, their densities are similar to those of gases. For instance, the best samples of silica aerogel have a density of about 2 mg cm^{-3} (density of air is 1.2 mg cm^{-3} in ambient conditions), which is 1000 times lower than that of nonporous solid materials. The density of graphene aerogel can be as low as 0.16 mg cm^{-3} (Ref. 114).

Besides, aerogels are characterized by very low thermal conductivity since the heat should pass through a highly branched network of thin chains formed by nanoparticles. Heat transfer in the air is also precluded because these chains make convection impossible.

Brittleness is the major drawback of aerogels. It is typical of almost all known silica aerogels, certain metal oxide aerogels and carbon aerogels. Nevertheless, preparation of aerogel based on graphene/carbon nanotube composite, with high elasticity and fracture strength was reported.[114]

Usually, graphene aerogels are prepared upon thickening of GO suspensions accompanied by partial reduction of GO and formation of a porous 3D network in the liquid. As the liquid phase is removed, a dry 3D graphene structure is available. Although GO-based aerogels offer certain advantages compared to conventional carbon aerogels, they are inferior in properties to the aerogels based on graphene nanosheets obtained by mechanical cleavage or by chemical vapour deposition, which are characterized by much higher crystallinity and superior mechanical and electrical characteristics.

Researchers from California University at Berkeley proposed a new method for the synthesis of aerogels from GO containing high-quality sheets of crystalline graphene.[94] The approach assumes the formation of a gel from a suspension of GO in aqueous ammonium hydroxide at a moderate temperature (~80 °C). The gel thus prepared is dried using supercritical carbon dioxide and then annealed at 1050 °C in nitrogen atmosphere. In this step, a conventional GO-based aerogel is formed. To prepare a highly crystalline gel, the process was augmented with annealing in helium atmosphere at temperatures above 1500 °C. High-resolution scanning electron microscopy (SEM) images demonstrate that the annealed gel is single-layer or few-layer highly crystalline graphene (Fig. 6). High-quality graphene sheets in the new aerogel provide its stability at high temperatures and exhibit higher strength and superior electrical properties compared to graphene in conventional graphene aerogels. The authors [94] believe that possible fields of application of the new material include catalysts and energy storage units, in particular, supercapacitors, lithium ion batteries, as well as devices for water desalination, sensors and composite materials.

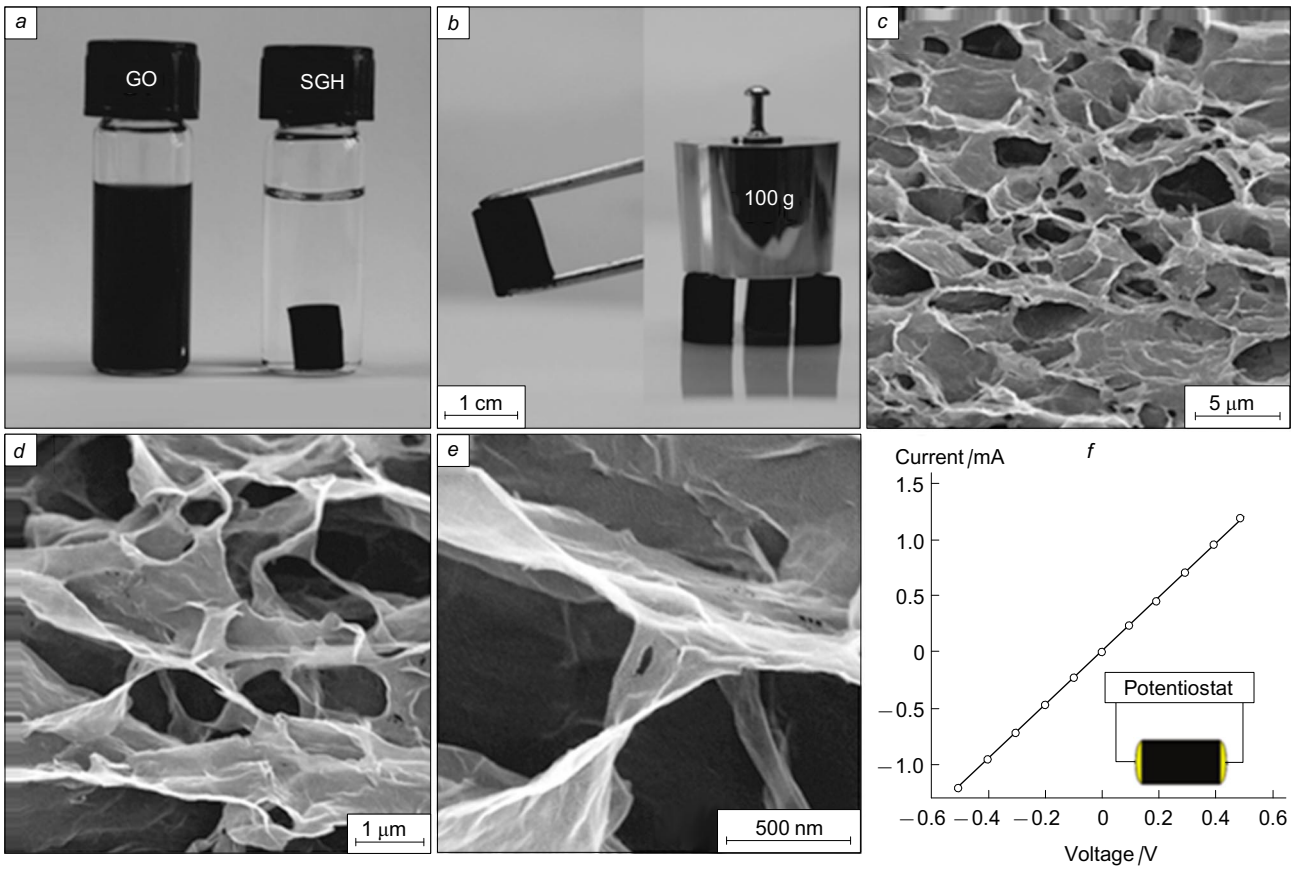


Figure 7. Photographs of graphene oxide aqueous dispersion (2 mg ml^{-1}) before and after hydrothermal reduction at 180 °C, 12 h (SGH is self-assembled graphene hydrogel) (*a*); photographs demonstrating high mechanical strength of aerogel (*b*); SEM images of the SGH interior structure at different magnification (*c*–*e*); room-temperature *I*–*V* curves for an aerogel (two-probe method) (*f*).[115]

A graphene aerogel was also prepared from GO hydrogel by hydrothermal synthesis (180 °C, 12 h) followed by vacuum freeze-drying.[115] The final monolith (aerogel) had a cellular macroporous structure with the framework formed through physiclal cross-linking of overlapping flexible graphene nanosheets. The aerogel demonstrated high mechanical and electrical properties (Fig. 7).

An rGO-based aerogel modified with silica nanoparticles was synthesized.[116] The porous material was highly hydrophobic (water contact angle of 137°) and had low density (13.5 mg cm^{-3}) and high specific surface area (516 $m^2\ g^{-1}$).

Yet another method for the preparation of graphene macroensembles uses rigid porous templates, *e.g.*, nickel foams.[117] Graphene is synthesized from CH_4 by chemical vapour deposition at ~1000 °C. The technique allows one to control the density of the solid phase by varying the amount of the deposited compound and the structure of the solid phase through the choice of the scaffold with the desired architecture, thus ensuring the attainment of high porosity and large specific surface area. However, the method requires high energy expenditure and is inappropriate for fabrication of self-supporting monoliths with high mechanical properties since the 3D networks break up with ease upon removal of rigid sacrificial framework.

Polystyrene and silica nanoparticles were also used as solid templates for the preparation of graphene monoliths with ordered porous structures.[75, 109, 111] However, this is possible either at high temperatures (above 800 °C) or in the presence of harmful chemical substances (*e.g.*, HF) to dissolve the solid SiO_2 scaffold. The use of other templates also significantly complicates the preparation of graphene architectures.

Fabrication of high-quality monoliths requires the development of chemistry of aqueous and organic 'solutions' of graphene derivatives.[63, 118, 119]

Almost all monoliths fabricated using the method described above (except methods that use solid templates and Pickering emulsions) have random porous structures formed by random stacking of 2D graphene nanosheets. Tuning the architecture of such 3D materials is a challenge. At present, fabrication of graphene monoliths with well-defined and controllable microstructures is impossible.[75] In this connection, the development of new approaches to the design of porous graphene materials with controllable architectures is required.

12. Graphene materials as methane sorbents

Methane is the main constituent of natural gas and plays an increasing role in power engineering. It is used in industry, in household, in boiler plants, as motor fuel and as raw material in chemical industry. The content of CH_4 in natural gas is about 90%, the overall concentration of other impurities being as high as 10 mass %; therefore, transformation of a natural gas storage facility to a methane storage facility requires gas separation.[120]

At the same time, a continuous decrease in the fraction of readily available fossil fuels necessitates a research into alternative energy sources including biogas.[121] For environmentally friendly use of biogas that is mainly composed of CH_4 and CO_2 it is necessary to develop efficient methods for separation of these gases.[122, 123]

Coalbeds represent yet another, at least equally important, source of methane. The action of high temperature and high pressure causes the formation of coalbed hydrocarbon gases with methane being the main component. The concentration of methane in the gas mixture is in the range of 80%–98%.[120]

Thus, the main problems related to utilization of methane include purification, transportation and storage.

In this review we will consider certain issues that are mainly related to the last-mentioned problem, *viz.*, application of porous adsorbents for methane collection.

An adsorption-based natural gas (methane) collection system is a storage unit specially filled with a porous adsorbent. Materials with high porosity and large specific surface area are promising for methane storage applications. The intermolecular forces acting between CH_4 molecule and an adsorbent are primarily induced by instant polarization of highly symmetric methane molecule. The interaction between the methane molecule and the pore wall is governed by the pore size.

A large surface area of an adsorbent provides high gravimetric methane uptake, while high volumetric methane uptake requires close packing. The packing density can be increased by compressing the powdered sample. The packing density should be considered as an important factor used to achieve high volumetric storage capacities of materials. A drawback of all powdered storage media is the packing density limitation equal to 0.3 g cm^{-3} for typical and 1 g cm^{-3} for an ideal bulk sample.

The Advanced Research Projects Agency-Energy (ARPA-E) of the US Department of Energy (DOE) reported the following target values of methane storage parameters: 0.5 g (CH_4) (g of sorbent)$^{-1}$ for the gravimetric density and 12.5 MJ (litre of sorbent)$^{-1}$ for the volumetric energy density in the temperature range from −40 to 85 °C for a vehicle under actual operating conditions.[124] Also, the packing losses of about ~25% and the sorbent price (less than 10 US dollars per kg) should be taken into account.

A number of recent reviews[125–137] on methane adsorption on porous solid graphene materials are available.

A comparative study of methane adsorption on typical carbon-based materials including graphene sheets, activated carbon and carbon black was reported.[127] It was shown that the adsorbed amount of methane does not change in proportion to the specific surface area of the adsorbent. Namely, the absolute adsorption at 0 °C and 20 bar was found to be 6 mmol g^{-1} on the activated carbon *vs.* 1.25 mmol g^{-1} on the graphene sheets and 0.6 mmol g^{-1} on the carbon black. However, the specific surface area of the activated carbon (1118 $m^2\ g^{-1}$) was nearly 3.7 and 14.6 times larger than that of the graphene sheets (300 $m^2\ g^{-1}$) and the carbon black (76 $m^2\ g^{-1}$), respectively. A similar conclusion was drawn from comparing the specific pore volumes of the adsorbents. Graphene nanosheets had larger specific pore volume compared to carbon black, but this did not lead to an increase in the storage volume per unit surface area, which was the largest for carbon black. It should be noted that microporosity of the graphene material mentioned above was not optimized. The efficiency of various porous adsorbents for CH_4 was compared elsewhere.[138, 139]

A detailed study of the interaction between methane and graphene is available.[128] According to calculations, the CH_4

molecule is oriented with three hydrogen atoms towards the graphene sheet, being located at a distance of 0.33 nm from the surface, and binding energy is 0.17 eV. Recently,[129] it was established that the equilibrium distance between the graphene surface and methane molecule is 0.31 nm and the corresponding adsorption energy is nearly 11.5 kJ mol^{-1}; this confirms weak interaction (physisorption) between CH_4 and graphene. Contrary to this, strong adsorption (chemisorption) of methane on Pt-decorated graphene was found when the CH_4 molecule was above a Pt atom on the graphene sheet. In this case, the calculated energy was nearly four times higher (46.8 kJ mol^{-1}) and the distance between the methane molecule and graphene was shorter (0.206 nm) as compared to the corresponding values obtained for undecorated graphene. The authors of yet another study[130] reported that edge functionalization of graphene can also favour methane adsorption.

Physisorption of CH_4 on modified graphene depends slightly on the orientation of methane molecules and on the electronegativity of the dopant atom.[140] For instance, doping graphene with boron decreases the adsorption energy of CH_4, whereas doping with nitrogen increases this energy. More intensive experimental studies in this field are needed to better understand the processes of adsorption on both pristine and doped graphene materials. It was reported that the measured methane adsorption capacity of activated S-doped rGO surface is only 0.5 mmol g^{-1} at 0 °C and 1 bar,[141] whereas doping a graphene aerogel with nitrogen causes its CH_4 adsorption capacity to increase from 1.4 mmol g^{-1} to 1.7 mmol g^{-1} under identical conditions.[142] At atmospheric pressure and 0 °C, a graphene material named graphene nanoribbon framework demonstrated a rather low methane adsorption capacity of 0.72 mmol g^{-1}. This can be a consequence of relatively small specific surface area (680 m^2 g^{-1}) as well as small micropore volume (0.16 cm^3 g^{-1}).[131] To attain higher CH_4 adsorption values, higher pressures are required.

A graphene nanomesh material characterized by high volumetric methane uptake of 200 cm^3(STP) cm^{-3} [where cm^3(STP) refers to the methane volume at the standard temperature (0 °C) and pressure (1 bar)] and high methane adsorption capacity (14.8 mmol g^{-1} at 1 °C and high pressure of 90 bar).[143] The material was synthesized by CVD using porous MgO sheets as a template and had a large specific surface area of 2038 m^2 g^{-1} with a pore size distribution centred at ~1 nm.

Moreover, as the bulk density of a graphene nanomesh pellet was increased to 0.5–1.0 g cm^{-3} by pressing, the volumetric methane uptake reached a value of 236 cm^3(STP) cm^{-3} at 1 °C and 90 bar. A drawback of this type of synthesis is a high consumption of valuable gaseous hydrocarbons to produce the final material. A 3D nanoporous graphene material (a-3D-G) characterized by a methane adsorption capacity of 12.03 mmol g^{-1} at 25 °C and a lower pressure (35 bar) was fabricated.[132] A large specific surface area of 2720 m^2 g^{-1} and a total pore volume of 1.45 cm^3 g^{-1} were obtained using alkali (KOH) activated graphene structure.

Yet another chemically activated graphene-based adsorbent is a-GDC, or graphene derived carbon.[144] The methane adsorption capacity of the material is 11.3 mmol g^{-1} at room temperature and 35 bar. It was also shown that a-GDC is a promising adsorbent for CO_2 (21 mmol g^{-1} at 25 °C and 20 bar) and H_2 (3.8 wt.% at −196 °C and 10 bar). High adsorption capacity of this material can be explained by the presence of well-developed porous structure with a BET specific surface area of 3240 m^2 g^{-1} with interconnected network of micro- and mesopores (average pore size of 2.75 nm). Besides, a-GDC is characterized by fast adsorption–desorption kinetics and low heat of adsorption, which indicates van der Waals interactions between the adsorbent surface and gas molecules. The pore size in this type of materials varied from 1 to 4 nm and the calculated optimum pore size for the most efficient methane capture at ambient temperature and 35 bar was 0.8–1.2 nm.[133] A GO-based carbon material a-GODC (graphene oxide derived carbon)[126] has a rather large BET specific surface area of 1900 m^2 g^{-1} and a total pore volume of 1.65 cm^3 g^{-1}. The methane adsorption capacity was 10.91 mmol g^{-1}. It was shown that the specific surface area, pore volume and the pore size distribution can be controlled by varying the concentration of the activator (KOH) solution and the treatment temperature.

In Fig. 8 we compare the methane adsorption properties of three graphene materials with different average pore sizes and specific surface areas (SSA) at 25 °C and 35 bar.[132, 137, 144] The structure parameters were calculated on the basis of low-temperature nitrogen adsorption isotherms. The effect of SSA on the methane uptake is not clearly seen, which can be due to the differences in the methods for evaluating the BET surface area. The same also holds for the effect of the pore diameter. However, based on the available adsorption data, one can assume that the pore size is a more important factor than SSA. In the range of average pore diameters from ~2.0 to ~2.8 nm the graphene adsorbents (see Fig. 8) are characterized by similar methane adsorption capacities ranging from ~10.9 to ~12.0 mmol g^{-1} despite a significant difference in their SSA (1900–3200 m^2 g^{-1}). To achieve higher CH_4 storage and efficient (fast) adsorption–desorption kinetics, it is required that the material have a large volume of optimum-size micropores and a certain volume of mesopores. The pore size distribution centred at 1 nm allows two or three CH_4 molecules to be accommodated within a pore, thus resulting in high packing density of the adsorbed phase.[133] According to calculations of the density of methane in micropores and micro-mesopores at pressures of up to 100 bar using experimental data for activated carbons,

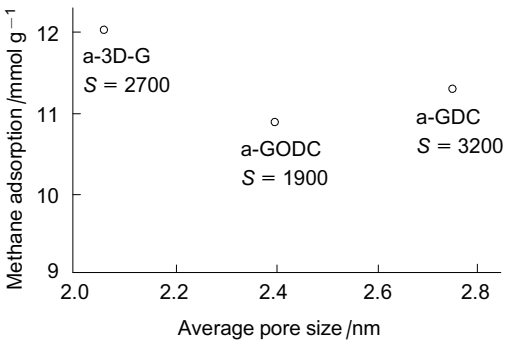


Figure 8. Methane adsorption capacities of three graphene materials at 25 °C and a pressure of 35 bar plotted *vs.* average pore size and Brunauer–Emmett–Teller specific surface area (*S*, expressed in m^2 g^{-1}).[125]

pores smaller than 1–2.5 nm in size have a strong effect on the methane adsorption capacity at high pressures.[134]

13. Methane adsorption on hybrid materials containing graphene derivatives and metal-organic frameworks

Although studies and application of metal-organic frameworks as methane storage units receive little attention compared to hydrogen storage[145] or CO_2 capture,[146] there has been gradually increasing activity in this field.

Peng *et al.*[147] determined that the US DOE gravimetric target for methane sorption can be reached using a MOF with an apparent surface area of 7500 $m^2\ g^{-1}$ and a pore volume of 3.2 $cm^3\ g^{-1}$. Based on these values of structural parameters, the volumetric methane uptake of this MOF should be 195 cm^3 (STP) cm^{-3}. The methane volumetric capacity of a well-studied and commercially available MOF known as a Hong Kong University of Science and Technology material (HKUST-1, MOF based on Cu^{2+} and benzene-1,3,5-tricarboxylic acid) can be as high as 267 cm^3 (STP) cm^{-3} at 25 °C and 65 bar and the single-crystal density of the sorbent. Since HKUST-1 has high storage capacity, can be synthesized with ease and is commercially available, it was proposed as a reference and to compare the properties of novel materials for methane storage units[136] with those of HKUST-1. A drawback of this material is low mechanical stability. Indeed, mechanical compaction leads to significant decrease in the volumetric capacity of HKUST-1.[147, 148] Recently, a similar MOF material with high volumetric methane uptake [16.58 mmol g^{-1} and 221 cm^3 (STP) cm^{-3} at 85 bar using a crystal density of 0.595 g cm^{-3}] was reported.[126] It was synthesized using highly aromatic and rigid organic linker with intrinsic strong CH_4 adsorption sites; the BET surface area of this material is 3971 $m^2\ g^{-1}$.

A comparison of the methane adsorption properties of various porous materials including activated carbons, MOF and graphene materials in relation to their SSA revealed[132] that MOF with SSA > 3000 $m^2\ g^{-1}$ exhibit saturation and thus a further increase in SSA should not improve their adsorption properties. At present, MOF and porous composites based on rGO attract increasing attention as methane adsorbents.[135, 149, 150] Figure 9 *b* presents a SEM image of the MOF/rGO hybrid material.[151] Although MOF have large specific surface area and well-developed porous structure, they are not always efficient adsorbents for light gas molecules at atmospheric pressure.[149]

Obtaining hybrid materials with high porosity and improved adsorption properties requires additional studies on the formation of graphene/MOF hybrids.[152, 153]

Zhou and co-workers[154] synthesized a rGO/MIL-101 hybrid [MIL is a Materials Institute Lavoisier material, a MOF based on benzene-1,4-dicarboxylic acid and chromium(III) cations] with a specific surface area of 2950 $m^2\ g^{-1}$ and a total pore volume of 1.42 $cm^3\ g^{-1}$. The material has a high methane adsorption capacity of 7.5 mmol g^{-1} at room temperature and 25 bar. A simulation performed for the rGO/MIL-101 system and equimolar $CO_2:CH_4$ mixture revealed high separation selectivity (15.0) at 1.5 bar (*cf.* an experimental separation selectivity of 32 at 1.5 bar for a mixture of 10% CO_2 and 90% CH_4).

For comparison, we present the data for activated carbons that are also considered as potential methane storage materials. For instance, activated carbons prepared from mesophase pitch adsorbed up to 160 cm^3 (STP) cm^{-3} of CH_4 at 25 °C and 35 bar and a packing density of 0.62 g cm^{-3} (Ref. 134). The adsorption capacity of KOH-activated carbon was 12.33 mmol g^{-1} at 20 °C and 50 bar.[155] A methane uptake of 10.25 mmol g^{-1} [147 cm^3(STP) cm^{-3}] at 25 °C and 20 bar attained for the carbon adsorbent AC4-PC (AC stands for activation, PC stands for porous carbon, KOH : PC = 4 mass %) is one of the best results reported for activated carbons with large surface area at relatively low pressures.[156] Activated carbons prepared in other studies[157, 158] were characterized by the following methane adsorption properties: 9.34 mmol g^{-1} [130 cm^3(STP) cm^{-3}] and 8.62 mmol g^{-1} [120 cm^3(STP) cm^{-3}] at 25 °C and ~30 bar, respectively.[157, 158]

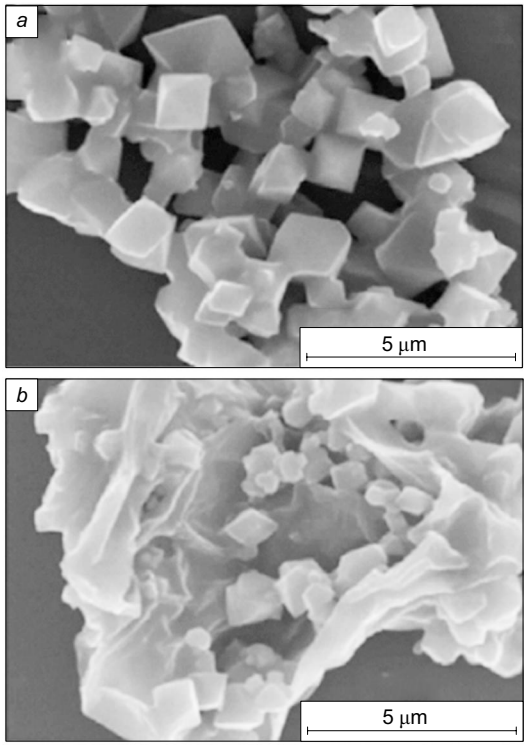


Figure 9. SEM images of materials based on metal-organic framework (*a*) and MOF/rGO hybrid (*b*).[151]

Zeolite 13X is often used as adsorbent because of its polar surface and large surface area and pore volume. The methane adsorption capacity of zeolite 13X is ~2.8 mmol g^{-1} at 30 °C and 10 bar, and the $CO_2:CH_4$ selectivity reaches a value of 26 at 30 °C and 4 bar.[159]

Table 2 presents the methane adsorption properties of various graphene-based materials. It should be noted that adsorption of CO_2 and H_2 on this type of materials has been much better studied than adsorption of CH_4.

Methane adsorption is usually measured at high pressures (> 20 bar). The values of adsorption at atmospheric pressure are taken from the gas separation studies. At high pressures, graphene materials along with MOF are the most promising methane adsorbents for potential commercial applications. For instance, graphene derivatives demonstrate high methane uptakes up to 12 mmol g^{-1} at 25 °C and pressures lower than 35 bar.[132] Further studies of

Table 2. Methane adsorption properties of graphene-based materials.

Graphene-based material	Pressure/ temperature (bar/°C)	Methane adsorption /mmol g^{-1}	Ref.
Graphene sheets	20/0	1.25	127
Nanomesh graphene	90/1	14.8	143
Graphene monolith	90/1	14.5	136
Spongy graphene	0.96/0	0.24	160
Graphene nanoribbon framework	1/0	0.72	131
a-GDC	35/25	11.3	144
a-GODC	35/27	10.91	137
a-3D-G	35/25	12.06	132
S-Doped graphene material	1/25	0.5	141
N-Doped graphene aerogel	1/0	1.74	142
rGO/MIL	25/25	7.5	154
Cu-MOF/rGO-1 [a]	1/0	~1.3	152
Cu-MOF/rGO-2 [a]	1.01/0	~1.3	153

[a] Cu-MOF are metal-organic frameworks based on Cu^{2+} and benzene-1,3,5-tricarboxylic acid.

methane adsorption on graphene-based materials, especially on activated graphene materials and rGO, which are characterized by high CO_2 and H_2 uptakes, are required.

14. Formation of porphyrin architectures on the surface of graphene materials. Covalent and noncovalent interactions in graphene – porphyrin hybrids

The main problem in the design of graphene-based hybrid materials is that pristine graphene exhibits very low solubility and aggregates through stacking of electron systems of the carbon framework. At present, all known approaches to the design of composite materials based on graphene derivatives and porphyrins involve, to one or another extent, preparation of graphene or GO dispersions.[161] In the case of graphene this often requires preliminary modification of the carbon framework. Chemical methods of preliminary exfoliation combine the use of strong acids,[77] ionic liquids,[162] surfactants[163] or organic solvents[164] and sonication.[165]

Subsequent covalent or noncovalent functionalization with various molecules or nanoparticles is carried out both in water and in nonaqueous solvents.[166 – 168]

Hybrid structures based on carbon materials and tetrapyrroles are fabricated using fundamental concepts of the interaction between tetrapyrrole aromatic platform and(or) functional substituents grafted to the porphyrin ring and the carbon substrate. Targeted design of such hybrid materials implies control of the porphyrin – substrate interactions and manipulation of the mobility and reactivity of the molecules involved. Depending on nature of the surface and on the structure of porphyrin molecular tectons, the organization of the porphyrins on the carbon substrate can vary following the combination of covalent and noncovalent bonds in the final structure. This variety of possibilities is to the full extent realized in the supramolecular structures based on porphyrins and their derivatives that have the advantage of chemical and thermal stability and variability of the molecular structures through grafting of substituents over other types of linkers used to assemble metal-organic frameworks.[169]

meso-Functionalization of porphyrins using appropriate substituents allows one to control assembly of nano- and microstructures on various surfaces. Substituents of low reactivity, such as phenyl groups (2*H*-tetraphenylporphyrin), mainly favour the formation of close-packed structures through van der Waals interactions and formation of the so-called T-shaped packing of substituents in adjacent molecules. Regular patterns of such structures are determined by the intrinsic lattice of the substrate.[170]

Incorporation of metals, *e.g.*, Fe, Co or Zn, into the porphyrin ring before or after assembling the supramolecular ensemble has almost no effect on the packing pattern.[171] Porphyrin units bearing bulky substituents (*e.g.*, *tert*-butylphenyl ones) form tetragonal[172] or close-packed hexagonal phases.[173, 174]

In order to graft MOF, the surface of graphene sheets can be functionalized with hydroxyl, aldehyde, carboxyl or epoxy groups by treating the surface with strong oxidants, *e.g.*, $KMnO_4 - H_2SO_4$ and then with H_2O_2. Exfoliation of the modified graphene is achieved by sonication of the material. Further chemical modification involves partial reduction of the GO surface using various agents, for instance, hydrazine to remove oxygen-containing groups and to reduce the conjugated structure in the carbon framework. Carboxylated GO is prepared by exfoliation in alkali medium followed by neutralization with HCl. This enables selective retention of carboxyl groups on the surface of the GO nanosheet. Functionalization of graphene and GO using stacking of porphyrins on 2D carbon frameworks has been studied in considerable detail.[175 – 178]

Covalent functionalization can also be achieved through cycloaddition of Pd porphyrin complexes to the carbon framework.[179] This type of graphene functionalization leads to the appearance of sp^3-defects in the carbon framework with simultaneous loss of conductive properties.[180]

In the vast majority of cases noncovalent functionalization is performed using planar aromatic molecules; as a consequence, the properties graphene are retained while its solubility increases owing to hydrophobic interactions and aromatic stacking.[181] Noncovalent functionalization of graphene and GO is achieved using porphyrins,[182, 183] phthalocyanines[184] and pyrenes.[185] Note that noncovalent functionalization of disperse GO and chemically reduced forms of GO in order to fabricate hybrid materials is mainly carried out using porphyrins capable of forming cationic species.[186 – 190] Usually, immobilization of porphyrins on the surface of carbon particles through stacking and electrostatic interactions accompanies mixing of the porphyrin and the carbon framework in the bulk of the disperse system.

Functional groups on the surface and at the edges of GO nanosheets play an important role in immobilization of porphyrins on GO particles. The most reliable method indicating successful immobilization is fluorescence spectroscopy since interactions between porphyrin and the graphene scaffold cause quenching of tetrapyrrole fluorescence through electron transfer or energy transfer from the excited state of the molecule to the electron

system of graphene.[190] Yet another informative method for monitoring the formation of the hybrid material is electronic absorption spectroscopy, which allows one to observe a bathochromic shift of the characteristic Soret band (strong band in the UV-vis spectra of porphyrins) when porphyrin interacts with GO. This shift is most pronounced for chemically modified GO and least pronounced for GO prepared by direct oxidative exfoliation.[191] Pyridyl-substituted porphyrins interact with the GO surface mainly through electrostatic forces, which allows one to evaluate the extent of immobilization from an increase in the efficiency of photoinduced electron transfer and(or) energy transfer from the organic material to the carbon framework.[182] Since the wettability of graphene and graphene derivatives depends on pH, the pH value can be preadjusted by adding amphiphilic block copolymer poly(isoprene-*b*-acrylic acid).[182, 192] This method affords stable aqueous dispersions of graphene and copolymer in anionic form in an alkali medium. Subsequent immobilization of cationic porphyrins on such a modified carbon framework followed by the formation of the hybrid material is also driven by electrostatic interactions between positively charged porphyrin and negatively charged GO nanosheets. The efficiency of immobilization of these composites, where porphyrin acts as photoexcited electron donor while the graphene sheet acts as electron acceptor can also be evaluated using photoluminescence spectroscopy and absorption spectroscopy.

Yet another method for immobilization of porphyrins on GO uses functionalized GO as a kind of a sheet-like surfactant, which enables the formation of adsorption layers at water–oil interfaces. Mixing of aqueous GO dispersions with porphyrin [*e.g.*, zinc 5,10,15,20-tetra(4-pyridyl)-21*H*,23*H*-porphine] solutions gives stable dispersed composites through interactions between the porphyrin and the GO adsorption layers.[193]

The surface porphyrin MOF was formed by modifying GO by grafting of bis-pyridyl groups as surface-anchored linkers for subsequent binding of MOF components.[177] The method enables the formation of stable dispersed composites with porous structure owing to the introduction of MOF crystallites and high electrocatalytic properties. Note that small amount of the carbon material in such composites severely restricts their use as gas sorbents.

An original method for MOF immobilization on the GO surface was practically implemented in our study.[194] It involves preliminary modification of GO nanosheets using metal salts that can act as metal cluster linkers both to ensure immobilization of porphyrins on the GO surface and to interconnect porphyrin linkers within the MOF. The method is characterized by variability of assembly conditions and chemical compositions of systems being assembled. It allows the surface MOF to be assembled in aqueous or water-emulsion media and involves the use of finely dispersed GO, which favours an increase in the specific surface area of the sorption surface of the material.

The strength, nature, directionality and selectivity of lateral intermolecular interactions in the porphyrin ensembles on the surface of solid substrates can be varied over a wide range using functional groups, *e.g.*, pyridyl,[195–202] nitrocarboxyl,[173, 203] alkoxy[204] or phenylarboxyl ones.[174] Owing to formation of intermolecular hydrogen bonds and(or) electrostatic intermolecular interactions the structure of supramolecular ensembles of functionalized porphyrins can vary from stacking aggregates,[173, 205] extended wires,[173, 204, 205] and porous networks[204, 206] to close-packed 2D layers.[195, 207]

Efficient assembly of metal porphyrins to ordered porous structures (MOF) on the surface occurs through metal–substituent coordination. These interactions allow one to fabricate extended linear[197, 198] and framework-type[198, 200, 201] supramolecular structures.

Considerable efforts have also been made to perform covalent assembly of framework structures to prepare more stable and strong nanosystems and supramolecular porous sorbents. A key problem in this field is to remove structural defects that negatively influence the uniform build-up and the properties of the framework structure porphyrin ensembles on the surface. Up to now such structures were mainly fabricated on the surface of noble metals by dehydrogenation of porphyrins. This procedure was used to synthesize covalently bound oligomers from unsubstituted free base porphyrins on an Ag(111) surface.[208] Bromine-substituted tetraarylporphyrins were covalently polymerized on Ag(111) surface using the Ullmann reaction activated by sublimation of porphyrins on the substrate and subsequent annealing of the substrate.[209] Optimization of this protocol depending on the assembly conditions using *trans*-substituted porphyrin [5,15-bis(4-bromophenyl)-10,20-bis-(4-iodophenyl)porphyrin] led to fabrication of extended chains, 2D frameworks and 3D porous heterostructures. In the case of iodo derivatives, lower activation energy of the reaction enabled the formation of extended 1D chains on solid substrate in the first stage of the assembly process. Subsequent thermal activation may induce transformation of these 1D domains into regularly patterned domains of covalently cross-linked 2D porous networks. Similar structures are formed using covalently bound dibromofluoro-substituted porphyrin oligomers.[210] A scanning electron microscopy (SEM) study showed that thermally activated *meso*-tetra(mesityl)porphyrin adsorbed on the Cu(110) surface undergoes homopolymerization.[211] Polymerization of Zn^{II} 10,20-diphenylporphyrin resulting in the formation of 1D ensembles was performed by successive polymerization on a similar substrate.[212]

A fundamentally different strategy for fabrication of porphyrin nanostructures on solid surfaces is based on *ex situ* synthesis of covalently bound fragments that are then applied to the surface of solid substrates using methods developed for non-subliming compounds, *e.g.*, using electrospray. It was used to obtain nanoring structures composed of ferrocene-bridged trisporphyrin building blocks. Nanorings built of 30 and 15 porphyrins form a ten- and a five-membered ring, respectively (Fig. 10).[213]

Ensembles with smaller pore size were fabricated using presynthetic assembly by Vernier templating[214] through formation of relatively small nano-rings (to 12-porphyrin nano-rings).

At present, the use of perfectly smooth solid layered substrates of atomic thickness, such as sp^2-hybridized graphene sheets, as platforms for controlled assembly of tetrapyrroles is one of the most promising and intensively developing areas.[215–217] Tetrapyrroles can be immobi-

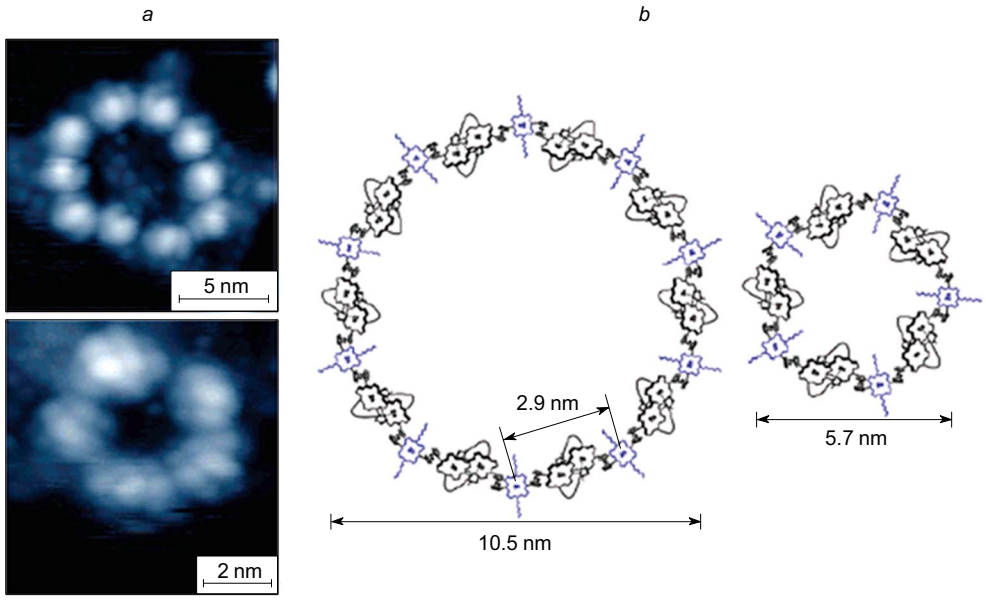


Figure 10. SEM images of ten- and five-membered nanorings of ferrocene-bridged trisporphyrin buildng blocks on an Au(111) surface in ultra-high vacuum at 77 K (*a*); the structure and dimensions of the deca- and pentamer (*b*).[213]

lized on such substrates by transfer of preliminarily ordered structures from metallic substrates to the graphite surface followed by exfoliation, as well as by direct self-assembly on modified 2D templates. Rigid C(sp^2) layers facilitate immobilization of the structures being assembled and thus ensure their assembly along the specified direction. It was shown that aromatic discotic molecules adsorbed from solution on the surface of CVD-graphene sheet on a Ru(0001) substrate can form an ordered close-packed monolayer.[217] A cobalt phthalocyanine complex forms close-packed hexagonal and tetragonal layers on graphene coated on a mixed substrate based on hexagonal boron nitride — (h-BN)SiO_2 (Ref. 215) or on Ir(111) surface.[218] The formation of organic tetrapyrrole islands is due to the templating effect of the (111) h-BN/Cu substrate for graphene. This effect manifests itself in the formation of a regular 2D Kagome lattice (trihexagonal packing) as the surface coverage increases. The Kagome lattice is formed due to spatial modulation of molecular orbitals on the extended electronic system of graphene.[216] Self-assembly and mechanical manipulation of porphyrin molecules on solid substrates is accompanied by other electronic effects influencing the behaviour of the molecules.[219]

Yet another possible route to stable close-packed porphyrin ensembles is to use compounds with grafted alkyl chains.[220] Tetrakis(alkoxyphenyl)porphyrin forms a lamellar packing on the HOPG surface, adopting a so-called 'face-on' orientation parallel to the carbon substrate and stabilized by intermolecular interpenetration of hydrocarbon substituents.[220] Carboxyl groups allow one to form porous patterns on graphite surface through formation of selective hydrogen bonds.[221] Liquid-phase self-assembly of porphyrin structures on the surface of carbon substrates can also be achieved using sulfonate groups.[222] Porous ensembles of more complex structure can be synthesized from solutions of double-decker or triple-decker sandwich porphyrin complexes,[223, 224] such as, *e.g.*, heteroleptic complex Ce(TPP-Fc)(C22OPP) (TPP-Fc is 5-[4-(4-ferrocenylphenylethynyl)phenyl]-10,15,20-triphenylporphyrin; C22OPP is 5,10,15,20-tetrakis(4-docosyloxyphenyl)porphyrin)[224] through hydrogen bonding, van der Waals interactions and $\pi-\pi$ stacking. Up to the present hybrid self-assembled porphyrin ensembles were mainly fabricated as potential fragments of photocatalytic devices.[225]

Photovoltaics and optoelectronics are rapidly developing areas of research into porphyrin/carbon hybrid materials; here, tetrapyrroles are used as electron donors. Of particular interest are composites based on tetrapyrroles and fullerenes or carbon nanotubes because they provide charge transfer from the tetrapyrrole moiety to the carbon scaffold. Monolayers of binary supramolecular composites based on C_{60} and porphyrins were prepared on different substrates.[226] Regular open framework structures formed by porphyrins enable immobilization of the carbon component immediately in the framework pores.[206] Supramolecular ensembles based on C_{60} and 5,15-bis(4-aminophenyl)-10,20-diphenylporphyrin and some other porphyrins can be transformed to covalently cross-linked copolymers by thermal anneling.[227–231] Supramolecular ensembles based on fullerene–porphyrin composites are also studied from the standpoint of transition from spontaneous assembly to a process controlled by external stimuli.[232] According to optical absorption spectroscopy, SEM and transmission electron microscopy data, noncovalent hybridization of porphyrins with single-wall nanotubes (SWNT) results in the formation of a 3D hybrid material with a framework architecture determined by the molecular structure of the porphyrins, the concentration of the hybrid and the SWNT : porphyrin ratio. The assembly of the hybrid material involves the formation of porphyrin J-aggregates on the outer surfaces of the SWNT with a tendency

to aggregation in porous ring structures. The presence of electron-donating pyridyl groups in *para*-positon of the phenyl rings in 5,10,15,20-tetraphenyl-21*H*,23*H*-porphine facilitates the formation of J-aggregates and the assembly of the porous superstructure based on SWNT.[233]

15. Composite materials based on porphyrins and graphene derivatives

Liquid-phase assembly of composites based on porphyrins and graphene derivatives offers prospects for fabrication of novel materials for catalytic, sorption, fuel cell, and other applications.

Usually, such an assembly proceeds following diverse and technologically simple protocols, although many factors should be taken into account. A particular advantage of liquid-phase assembly is that it can be used when electrodeposition or sublimation from the gas phase is impossible. Structures assembled at the liquid–solid interface are formed either under the action of weak forces between the carbon substrate and porphyrin molecules or through specific interactions between functional groups and the surface.[232, 234–236]

Control of these interactions made it possible to develop a new method for the preparation of graphene from graphite using liquid-phase porphyrin exfoliation of graphite. Graphite is pretreated with organic ammonium bases to give an intercalated scaffold and then porphyrins capable of incorporating into the hybrid material through stacking interactions with the graphene sheets are introduced. Graphene sheets thus obtained have undisturbed sp^2 carbon structure.[183, 237]

At present, the application of graphene–porphyrin composites is limited to a few areas,[238] in particular, sorption and extraction of heavy metal salts. Such composites were used as solid-phase adsorbents for preconcentration and extraction of Zn^{II} from aqueous solutions.[238] However, the primary practical interest in this type of materials is first of all associated with electro- and photocatalysis. A typical example is provided by electrochemical reduction and functionalization of GO nanoribbons using a water-soluble complex, Fe^{III} *meso*-tetrakis(*N*-methyl-4-pyridinio)porphyrin (FeTMPyP), through noncovalent π–π interactions resulting in the formation of aggregated sp^2-hybridized domains on the electrode surface.[239] Hybrid films thus fabricated demonstrate very high electrocatalytic characteristics in the reduction of dissolved oxygen. These films were applied in a biosensor for fast amperometric detection of glucose.

Photocatalytic oxidation of rhodamine B was carried out using a hybrid material with developed internal porous structure based on GO and a zinc complex of tetrapyridyl-substituted porphyrin. In this composite, GO simultaneously acts as surfactant promoting the assembly of the supramolecular hybrid structure and as the functional component responsible for efficient synergistic photooxidation of substrate.[193]

Cobalt porphyrin Co^{2+}-THPP [THPP is 5,10,15,20-tetrakis(4-hydroxyphenyl)porphyrin] and rGO were used to synthesize novel electrocatalytic materials for oxygen reduction from carbon dioxide with the chemical composition rGO/(Co^{2+}-THPP)$_n$. Preparation of the graphene–poprphyrin catalytic material using the layer-by-layer assembly is schematically shown in Fig. 11. Compared to other GO-based carbon materials including scaffolds modified with cobalt salts, these hybrid materials exhibit much higher catalytic activity comparable with that of the best commercially available Pt/C catalysts. However, the hybrid catalysts are more stable owing to fine tuning of the structure and maximization of the synergistic action of both components.[235]

Porphyrin–graphene composites are of interest as materials for nonlinear optics. Novel covalently functionalized composites GO–(Cu, Zn, Sn, H_2, VO)-porphyrin[240] are characterized by strong quenching of porphyrin fluorescence, which is indicative of the interaction between the tetrapyrrole ring and the graphene scaffold. These composites exhibit nonlinear optical properties observed in the studies of absorption using

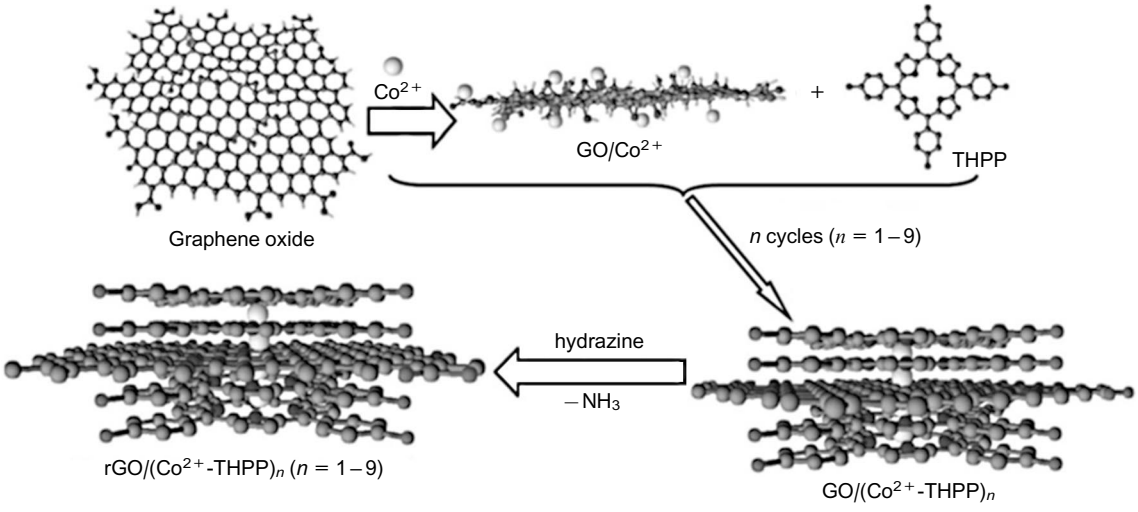


Figure 11. Preparation of graphene–porphyrin catalytic material rGO/(Co^{2+}-THPP)$_n$ using the layer-by-layer assembly technique.[235]

femtosecond laser pulses; the most pronounced nonlinear effects were observed for the composite based on the free base porphyrin.

So-called nanohybrid materials for nonlinear optics were prepared using rGO pre-modified with diazonium salts and porphyrins. In this case, modification enables covalent grafting of porphyrins to the surface of the carbon material. Immobilization of porphyrins on the rGO surface significantly increases the solubility and processability of rGO and rGo-based materials. A feature of this type of materials is efficient photoinduced electron transfer and(or) energy transfer from the tetrapyrrole rings to the extended π-system of rGO owing to interactions between the carbon scaffold and porphyrin. As a consequence, these materials exhibit much better nonlinear optical properties than not only their individual components, but also conventional materials based on C_{60} fullerene.[241]

In spite of rapid progress in the chemistry of porphyrin/carbon composite materials, there are only a few publications on the design of MOF/graphene composites based on tetrapyrrole linkers. Note that most systems in question are also considered as catalysts for various processes. The development of methods for fabrication of such materials is an innovation area of basic and applied research.

In particular, graphene nanoribbons (GNR) were used as templates to incorporate with the metal-organic framework MOF-525 based on Zr^{IV} and carboxyl-substituted porphyrin [5,10,15,20-tetrakis(4-carboxyphenyl)-porphyrin] by solvothermal synthesis in aqueous dispersion of GNR.[242] The framework structure of the composite is composed of MOF nanocrystals interconnected by 1D nanoribbons. The material was used to prepare an electrochemical catalyst for the decomposition of nitrites. Highly porous MOF nanocrystals acted as the catalyst while the GNR network ensured fast and efficient charge transfer. The composite was shown to be a much more efficient catalyst compared to analogous MOFs.

Yet another example of assembly of a porphyrin MOF on a graphene substrate is provided by iron porphyrin complexes formed on rGO pre-modified with bis-pyridyl ligands for subsequent surface immobilization of porphyrin molecules. It was shown that the composite material thus fabricated can be used as synergistic catalyst for electrochemical reduction of oxygen from water, thus being a cheaper and readily available alternative to platinum electrodes for fuel cells.[177] Besides, this type of composites can be used for the oxidation of cyclohexane at 150 °C.[243]

No porphyrin MOF on graphene substrates used as gas sorbents have been reported to date. Based on analysis of published data, one can suggest that composites based on porphyrin MOF and graphene aerogels are the most promising for application as selective membrane cleaners and separators for sorption of carbon dioxide and(or) hydrogen sulfide and purification of methane in the thin outer layer of sorbents when pumping the gas into storage facilities. Economic and efficient purification of natural gas from bound carbonic acid and hydrogen sulfide using selective sorbents is a crucial task for gas producing industry since carbonic acid residue formed during gas liquefaction precludes its utilization and transportation. Environmental risks associated with production of graphene – MOF composite materials can be minimized since graphene aerogel is a green material while potentially toxic or contaminating MOF components are used in small amounts relative to the overall volume of the composite material.

16. Conclusion

Studies on the synthesis and properties of and graphene derivatives are one of the most demanded and rapidly progressing areas in chemistry and physics. Increasing interest in this class of novel materials is, in particular, due to the possibility to fabricate monolithic hybrid porous structures. Chemical liquid-phase approaches ('soft' chemistry methods) to the synthesis of these materials considered in this review offer the advantages of large-scale production and relatively simple and available methods for modification of the structure and properties depending on the field of application. Colloidal dispersions (hydro- and organosols) of graphene derivatives are convenient systems for performing various technological steps including mixing, dispersion, impregnation, functionalization, gelation, *etc.*, that are necessary to fabricate the target products. Numerous studies are aimed to prepare GO hydrogels and treat them using physicochemical methods in order to assemble 3D architectures (*e.g.*, rGO aerogels). Aerogels prepared from such precursors as Pickering emulsions stabilized by graphene derivatives enable the formation of homogeneous porous monoliths.

Considerable attention paid to scientific research into the design of novel promising graphene-based adsorbents is due to sustainable need to develop efficient methods for storage and transportation of natural energy sources, in particular, methane. Although at present graphene derivatives are characterized by rather low methane uptake, it seems likely that the results obtained can be improved by incorporating MOF into graphene scaffolds. Clearly, further studies aimed to improve the properties of hybrid materials are required.

Recent publications have a high impact on the design of carbon material/porphyrin hybrids. These studies are based on fundamental concepts of the interaction between the tetrapyrrole aromatic platform and(or) functional substituents grafted to the porphyrin ring and the graphene substrate. Liquid-phase assembly of porphyrin/graphene composites offers prospects for fabrication of novel materials for catalytic, sorption, fuel cell, and other applications. Porphyrin MOF/graphene aerogel composites can be used as selective membrane cleaners and separators for sorption of carbon dioxide and(or) hydrogen sulfide and purification of methane in the thin outer layer of sorbents when pumping the gas into storage facilities.

The review has been written with the financial support from the Gazprom JSC.

Figures 4, 8, 9 are courtesy of Elsevier. Figures 5, 11 are courtesy of Wiley Interscience. Figures 6, 7, 10 are courtesy of the American Chemical Society.

References

1. S.Ahn, J.S.Sung, H.Kim, Y.Sung. *J. Mater. Sci. Eng.*, **4**, 192 (2015)
2. R.Mas-Balleste, C.Gómez-Navarro, J.Gómez-Herrero, F.Zamora. *Nanoscale*, **3**, 20 (2011)
3. F.Kang, Y.-P.Zheng, H.-N.Wang, Y.Nishi, M.Inagaki. *Carbon*, **40**, 1575 (2002)
4. B.J.Lee. *Bull. Korean Chem. Soc.*, **23**, 1801 (2002)
5. A.T.Dideikin, V.V.Sokolov, D.A.Sakseev, M.B.Baidakova, A.Ya.Vul'. *Tech. Phys.*, **55**, 1378 (2010)
6. K.S.Novoselov, A.K.Geim, S.V.Morozov, D.Jiang, Y.Zhang, S.V.Dubonos, I.V.Grigorieva, A.A.Firsov. *Science*, **306**, 666 (2004)
7. S.Nardecchia, D.Carriazo, M.L.Ferrer, M.C.Gutiérrez, F.del Monte. *Chem. Soc. Rev.*, **42**, 794 (2013)
8. K.S.Novoselov, A.K.Geim. The Nobel Prize in Physics 2010: https://www/nobelprize.org/prizes/physics/2010/summary/ (accessed 24.08.2019)
9. *Nanoscience and Technology: A Collection of Reviews from Nature Journals*. (Eds P.Rodgers, J.Heath). (London: World Scientific, 2010)
10. P.Blake, E.W.Hill, A.H.Castro Neto, K.S.Novoselov, D.Jiang, R.Yang, T.J.Booth, A.K.Geim. *Appl. Phys. Lett.*, **91**, 063124 (2007)
11. G.Chen, W.Weng, D.Wu, C.Wu, J.Lu, P.Wang, X.Chen. *Carbon*, **42**, 753 (2004)
12. A.E.Teplykh, S.G.Bogdanov, Yu.A.Dorofeev, A.N.Pirogov, Yu.N.Skryabin, V.G.Makotchenko, A.S.Nazarov, V.E.Fedorov. *Crystallogr. Rep.*, **51**, S62 (2006)
13. M.P.Poverennaya. Grafenovyi Bum. Itogi. (Graphenw Boom. Results). (Electronic Resource URL: http://www.nanometer.ru/2012/10/26/13512365078102_298275.html) (accessed 24.08.2019)
14. S.Bae, H.Kim, Y.Lee, X.Xu, J.-S.Park, Y.Zheng, J.Balakrishnan, T.Lei, H.R.Kim, Y.I.Song, Y.-J.Kim, K.S.Kim, B.Özyilmaz, J.-H.Ahn, B.H.Hong, S.Iijima. *Nat. Nanotech.*, **5**, 574 (2010)
15. G.Ruan, Z.Sun, Z.Peng, J.M.Tour. *ACS Nano*, **5**, 7601 (2011)
16. L.Banszerus, M.Schmitz, S.Engels, J.Dauber, M.Oellers, F.Haupt, K.Watanabe, T.Taniguchi, B.Beschoten, C.Stampfer. *Sci. Adv.*, **1**, e1500222 (2015)
17. J.J.Wang, M.Y.Zhu, R.A.Outlaw, X.Zhao, D.M.Manos, B.C.Holloway, V.P.Mammana. *Appl. Phys. Lett.*, **85**, 1265 (2004)
18. F.Parvizi, D.Teweldebrhan, S.Ghosh, I.Calizo, A.A.Balandin, H.Zhu, R.Abbaschian. *Micro Nano Lett.*, **3**, 29 (2008)
19. K.S.Novoselov, V.I.Fal, L.Colombo, P.R.Gellert, M.G.Schwab, K.Kim. *Nature (London)*, **490**, 192 (2012)
20. G.Brumfiel. *Nature (London)*, **458**, 390 (2009)
21. *Graphene Nanoelectronics: From Materials to Circuits*. (Ed. R.Murali). (New York: Springer, 2012)
22. L.A.Chernozatonskii, P.B.Sorokin, A.A.Artukh. *Russ. Chem. Rev.*, **83**, 251 (2014)
23. V.Singh, D.Joung, L.Zhai, S.Das, S.I.Khondaker, S.Seal. *Prog. Mater. Sci.*, **56**, 1178 (2011)
24. *Graphene Nanoelectronics: Metrology, Synthesis, Properties, and Applications*. (Ed. H.Raza). (Berlin, Heidelberg: Springer, 2012)
25. B.C.Brodie. *Phil. Trans. R. Soc. London*, **149**, 249 (1859)
26. S.Pei, H.-M.Cheng. *Carbon*, **50**, 3210 (2012)
27. S.P.Gubin, S.V.Tkachev. *Radioelectronics. Nanosystems. Inform. Technol. (RENSIT)*, **2**, 91 (2010)
28. W.Gao, L.B.Alemany, L.Ci, P.M.Ajayan. *Nat. Chem.*, **1**, 403 (2009)
29. M.Acik, G.Lee, C.Mattevi, A.Pirkle, R.M.Wallace, M.Chhowalla, K.Cho, Y.Chabal. *J. Phys. Chem. C*, **115**, 19761 (2011)
30. A.Bonanni, A.Ambrosi, M.Pumera. *Chem. – Eur. J.*, **18**, 4541 (2012)
31. D.R.Dreyer, A.D.Todd, C.W.Bielawski. *Chem. Soc. Rev.*, **43**, 5288 (2014)
32. O.C.Compton, S.T.Nguyen. *Small*, **6**, 711 (2010)
33. A.Buchsteiner, A.Lerf, J.Pieper. *J. Phys. Chem. B*, **110**, 22328 (2006)
34. L.Zhang, J.Liang, Y.Huang, Y.Ma, Y.Wang, Y.Chen. *Carbon*, **47**, 3365 (2009)
35. C.Hontoria-Lucas, A.J.López-Peinado, J.de D.López-González, M.L.Rojas-Cervantes, R.M.Martín-Aranda. *Carbon*, **33**, 1585 (1995)
36. N.V.Medhekar, A.Ramasubramaniam, R.S.Ruoff, V.B.Shenoy. *ACS Nano*, **4**, 2300 (2010)
37. R.C.Croft. *Chem. Soc. Rev.*, **14**, 1 (1960)
38. W.S.Hummers Jr., R.E.Offeman. *J. Am. Chem. Soc.*, **80**, 1339 (1958)
39. C.Petit, M.Seredych, T.J.Bandosz. *J. Mater. Chem.*, **19**, 9176 (2009)
40. Y.H.Ding, P.Zhang, Q.Zhuo, H.M.Ren, Z.M.Yang, Y.Jiang. *Nanotechnology*, **22**, 215601 (2011)
41. H.Sun, Y.Yang, Q.Huang. *Integr. Ferroelectr.*, **128**, 163 (2011)
42. O.Akhavan, E.Ghaderi. *J. Phys. Chem. C*, **113**, 20214 (2009)
43. C.-Y.Su, Y.Xu, W.Zhang, J.Zhao, X.Tang, C.-H.Tsai, L.-J.Li. *Chem. Mater.*, **21**, 5674 (2009)
44. D.C.Marcano, D.V.Kosynkin, J.M.Berlin, A.Sinitskii, Z.Sun, A.Slesarev, L.B.Alemany, W.Lu, J.M.Tour. *ACS Nano*, **4**, 4806 (2010)
45. N.I.Kovtyukhova, P.J.Ollivier, B.R.Martin, T.E.Mallouk, S.A.Chizhik, E.V.Buzaneva, A.D.Gorchinskiy. *Chem. Mater.*, **11**, 771 (1999)
46. G.Shao, Y.Lu, F.Wu, C.Yang, F.Zeng, Q.Wu. *J. Mater. Sci.*, **47**, 4400 (2012)
47. S.Kim, S.Zhou, Y.Hu, M.Acik, Y.J.Chabal, C.Berger, W.De Heer, A.Bongiorno, E.Riedo. *Nat. Mater.*, **11**, 544 (2012)
48. B.C.Brodie. *Ann. Chim. Phys.*, **59**, 466 (1860)
49. L.C.Staudenmaier. *Ber. Dtsch. Chem. Ges.*, **31**, 1481 (1898)
50. S.Stankovich, D.A.Dikin, R.D.Piner, K.A.Kohlhaas, A.Kleinhammes, Y.Jia, Y.Wu, S.T.Nguyen, R.S.Ruoff. *Carbon*, **45**, 1558 (2007)
51. X.Fan, W.Peng, Y.Li, X.Li, S.Wang, G.Zhang, F.Zhang. *Adv. Mater.*, **20**, 4490 (2008)
52. H.Wang, J.T.Robinson, X.Li, H.Dai. *J. Am. Chem. Soc.*, **131**, 9910 (2009)
53. C.Nethravathi, M.Rajamathi. *Carbon*, **46**, 1994 (2008)
54. O.Akhavan. *Carbon*, **48**, 509 (2010)
55. Y.Zhou, Q.Bao, L.A.L.Tang, Y.Zhong, K.P.Loh. *Chem. Mater.*, **21**, 2950 (2009)
56. Y.Zhu, S.Murali, M.D.Stoller, A.Velamakanni, R.D.Piner, R.S.Ruoff. *Carbon*, **48**, 2118 (2010)
57. W.Chen, L.Yan. *Nanoscale*, **2**, 559 (2010)

58. E.P.Neustroev, G.N.Aleksandrov, M.V.Nogovitsyna. *Vestn. North-Eastern Federal Univ.*, **6**, 87 (2015)
59. W.Chen, L.Yan, P.R.Bangal. *Carbon*, **48**, 1146 (2010)
60. H.-L.Guo, X.-F.Wang, Q.-Y.Qian, F.-B.Wang, X.-H.Xia. *ACS Nano*, **3**, 2653 (2009)
61. S.V.Tkachev. Candidate Thesis in Chemical Sciences, IGIC RAS, Moscow, 2012
62. S.Eigler, A.Hirsch. *Angew. Chem., Int. Ed.*, **53**, 7720 (2014)
63. E.D.Grayfer, V.G.Makotchenko, A.S.Nazarov, S.-J.Kim, V.E.Fedorov. *Russ. Chem. Rev.*, **80**, 751 (2011)
64. J.Liu, J.Tang, J.J.Gooding. *J. Mater. Chem.*, **22**, 12435 (2012)
65. F.M.Koehler, A.Jacobsen, K.Ensslin, C.Stampfer, W.J.Stark. *Small*, **6**, 1125 (2010)
66. G.Goncalves, P.A.A.P.Marques, C.M.Granadeiro, H.I.S.Nogueira, M.K.Singh, J.Grácio. *Chem. Mater.*, **21**, 4796 (2009)
67. E.Bekyarova, S.Sarkar, S.Niyogi, M.E.Itkis, R.C.Haddon. *J. Phys. D: Appl. Phys.*, **45**, 154009 (2012)
68. J.-Y.Hong, J.-Y.Wie, Y.Xu, H.S.Park. *Phys. Chem. Chem. Phys.*, **17**, 30946 (2015)
69. J.Greenwood, T.H.Phan, Y.Fujita, Z.Li, O.Ivasenko, W.Vanderlinden, H.van Gorp, W.Frederickx, G.Lu, K.Tahara, Y.Tobe, H.Uji-i, S.Fl Mertens, S.De Feyter. *ACS Nano*, **9**, 5520 (2015)
70. A.B.Bourlinos, D.Gournis, D.Petridis, T.Szabó, A.Szeri, I.Dékány. *Langmuir*, **19**, 6050 (2003)
71. R.Sharma, J.H.Baik, C.J.Perera, M.S.Strano. *Nano Lett.*, **10**, 398 (2010)
72. *Graphene Oxide: Reduction Recipes, Spectroscopy, and Applications*. (Ed. W.Gao). (Cham: Springer, 2015)
73. D.Chen, H.Feng, J.Li. *Chem. Rev.*, **112**, 6027 (2012)
74. Y.Hernandez, M.Lotya, D.Rickard, S.Bergin, J.N.Coleman. *Langmuir*, **26**, 3208 (2009)
75. P.C.Sherrell, C.Mattevi. *Mater. Today*, **19**, 428 (2016)
76. X.Zheng, H.Lee, T.H.Weisgraber, M.Shusteff, J.DeOtte, E.B.Duoss, J.D.Kuntz, M.M.Biener, Q.Ge, J.A.Jackson, S.O.Kucheyev, N.X.Fang, C.M.Spadaccini. *Science*, **344**, 1373 (2014)
77. S.Park, R.S.Ruoff. *Nat. Nanotech.*, **4**, 217 (2009)
78. J.I.Paredes, S.Villar-Rodil, A.Martínez-Alonso, J.M.D.Tascon. *Langmuir*, **24**, 10560 (2008)
79. A.G.Bannov, A.A.Timofeeva, V.V.Shinkarev, K.D.Dyukova, A.V.Ukhina, E.A.Maksimovskii, S.I.Yusin. *Prot. Met. Phys. Chem.*, **50**, 183 (2014)
80. M.Hirata, T.Gotou, S.Horiuchi, M.Fujiwara, M.Ohba. *Carbon*, **42**, 2929 (2004)
81. T.Szabó, A.Szeri, I.Dékány. *Carbon*, **43**, 87 (2005)
82. W.Cai, R.D.Piner, F.J.Stadermann, S.Park, M.A.Shaibat, Y.Ishii, D.Yang, A.Velamakanni, S.J.An, M.Stoller, D.Chen, R.S.Ruoff. *Science*, **321**, 1815 (2008)
83. T.Szabó, O.Berkesi, I.Dékány. *Carbon*, **43**, 3186 (2005)
84. T.Szabó, O.Berkesi, P.Forgó, K.Josepovits, Y.Sanakis, D.Petridis, I.Dékány. *Chem. Mater.*, **18**, 2740 (2006)
85. D.Li, M.B.Müller, S.Gilje, R.B.Kaner, G.G.Wallace. *Nat. Nanotechnol.*, **3**, 101 (2008)
86. X.Sun, Z.Liu, K.Welsher, J.T.Robinson, A.Goodwin, S.Zaric, H.Dai. *Nano Res.*, **1**, 203 (2008)
87. O.C.Compton, Z.An, K.W.Putz, B.J.Hong, B.G.Hauser, L.C.Brinson, S.T.Nguyen. *Carbon*, **50**, 3399 (2012)
88. S.Wang, L.A.ling Tang, Q.Bao, M.Lin, S.Deng, B.M.Goh, K.P.Loh. *J. Am. Chem. Soc.*, **131**, 16832 (2009)
89. C.-J.Shih, S.Lin, R.Sharma, M.S.Strano, D.Blankschtein. *Langmuir*, **28**, 235 (2011)
90. R.L.D.Whitby, V.M.Gun'ko, A.Korobeinyk, R.Busquets, A.B.Cundy, K.László, J.Skubiszewska-Zięba, R.Leboda, E.Tombácz, I.Y.Toth, K.Kovacs, S.V.Mikhalovsky. *ACS Nano*, **6**, 3967 (2012)
91. Yu.M.Shul'ga, S.A.Baskakov, A.D.Zolotarenko, E.N.Kabachkov, V.E.Muradyan, D.N.Voilov, V.A.Smirnov, V.M.Martynenko, D.V.Shchur, A.P.Pomytkin. *Nanosistemi, Nanomateriali, Nanotehnologii,* **11**, 161 (2013)
92. Y.Xu, G.Shi. *J. Mater. Chem.*, **21**, 3311 (2011)
93. C.Li, G.Shi. *Nanoscale*, **4**, 5549 (2012)
94. M.A.Worsley, T.T.Pham, A.Yan, S.J.Shin, J.R.I.Lee, M.Bagge-Hansen, W.Mickelson, A.Zettl. *ACS Nano*, **8**, 11013 (2014)
95. Y.Ma, Y.Chen. *Natl. Sci. Rev.*, **2**, 40 (2015)
96. F.Liu, T.Seo. *Adv. Funct. Mater.*, **20**, 1930 (2010)
97. Z.Sui, X.Zhang, Y.Lei, Y.Luo. *Carbon*, **49**, 4314 (2011)
98. K.-X.Sheng, Y.-Xi Xu, L.Chun, G.-q.Shi. *New Carbon Mater.*, **26**, 9 (2011)
99. C.Li, G.Shi. *Adv. Mater.*, **26**, 3992 (2014)
100. F.Kim, L.J.Cote, J.Huang. *Adv. Mater.*, **22**, 1954 (2010)
101. J.-J.Shao, W.Lv, Q.-H.Yang. *Adv. Mater.*, **26**, 5586 (2014)
102. S.U.Pickering. *J. Chem. Soc.*, **91**, 2001 (1907)
103. W.Ramsden. *Proc. R. Soc. London*, **72**, 156 (1904)
104. E.V.Ermakova, Yu.Yu.Enakieva, I.N.Meshkov, A.E.Baranchikiv, A.I.Zvyagina, Yu.G.Gorbunov, A.Yu.Tzivadze, M.A.Kalinina, V.V.Arslanov. *Makrogeterotsikly*, **10**, 496 (2017)
105. Y.He, F.Wu, X.Sun, R.Li, Y.Guo, C.Li, L.Zhang, F.Xing, W.Wang, J.Gao. *ACS Appl. Mater. Interfaces*, **5**, 4843 (2013)
106. H.Wang, J.Liu, H.Xu, Z.Ma, W.Jia, S.Ren. *RSC Adv.*, **6**, 106297 (2016)
107. K.Hu, X.Xie, M.Cerruti, T.Szkopek. *Langmuir*, **31**, 5545 (2015)
108. G.Yin, Z.Zheng, H.Wang, Q.Du, H.Zhang. *J. Colloid Interface Sci.*, **394**, 192 (2013)
109. P.Xie, X.Ge, B.Fang, Z.Li, Y.Liang, C.Yang. *Colloid Polym. Sci.*, **291**, 1631 (2013)
110. S.I.Kattimuttathu, C.Krishnappan, V.Vellorathekkaepadil, R.Nutenki, V.R.Mandapati, M.Černik. *Polym. Adv. Technol.*, **26**, 214 (2015)
111. X.Fei, L.Xia, M.Chen, W.Wei, J.Luo, X.Liu. *Materials*, **9**, 731 (2016)
112. K.P.Loh, Q.Bao, P.K.Ang, J.Yang. *J. Mater. Chem.*, **20**, 2277 (2010)
113. A.C.Pierre, G.M.Pajonk. *Chem. Rev.*, **102**, 4243 (2002)
114. H.Sun, Z.Xu, C.Gao. *Adv. Mater.*, **25**, 2554 (2013)
115. Y.Xu, K.Sheng, C.Li, G.Shi. *ACS Nano*, **4**, 4324 (2010)
116. X.Wu, J.Lyu, G.Hong, X.-c.Liu, X.Zhang. *Langmuir*, **34**, 9004 (2018)
117. Z.Chen, W.Ren, L.Gao, B.Liu, S.Pei, H.-M.Cheng. *Nat. Mater.*, **10**, 424 (2011)
118. S.Park, D.Dikin, S.T.Nguyen, R.S.Ruoff. *J. Phys. Chem. C*, **113**, 15801 (2009)
119. H.Kim, A.A.Abdala, C.W.Macosko. *Macromolecules*, **43**, 6515 (2010)
120. V.A.Sokolov, M.A.Bestuzhev, T.V.Tikhomolova. *Khimicheskii Sostav Neftei i Prirodnykh Gazov v Svyazi s ikh Proiskhozhdeniem*. (Chemical Composition of Oil and Natural Gases Related to their Origin). (Moscow: Nedra, 1972)

121. J.D.Murphy, E.McKeogh, G.Kiely. *Appl. Energy*., **77**, 407 (2004)
122. J.-J.Chen, W.-W.Li, X.-L.Li, H.-Q.Yu. *Environ. Sci. Technol*., **46**, 10341 (2012)
123. A.Hassani, M.T.H.Mosavian, A.Ahmadpour, N.Farhadian. *J. Chem. Phys*., **142**, 234704 (2015)
124. Methane Opportunities for Vehicular Energy (MOVE). DE-FOA-0000672, EUA (2012); https://arpa-e-foa.energy.gov (accessed 24.08.2019)
125. B.Szczęśniak, J.Choma, M.Jaroniec. *Adv. Colloid Interface Sci*., **243**, 46 (2017)
126. I.Spanopoulos, C.Tsangarakis, E.Klontzas, E.Tylianakis, G.Froudakis, K.Adil, Y.Belmabkhout, M.Eddaoudi, P.N.Trikalitis. *J. Am. Chem. Soc*., **138**, 1568 (2016)
127. Z.W.Zhu, Q.R.Zheng. *Appl. Therm. Eng*., **108**, 605 (2016)
128. C.Thierfelder, M.Witte, S.Blankenburg, E.Rauls, W.G.Schmidt. *Surf. Sci*., **605**, 746 (2011)
129. A.S.Rad, H.Pazoki, S.Mohseni, D.Zareyee, M.Peyravi. *Mater. Chem. Phys*., **182**, 32 (2016)
130. V.S.Kandagal, A.Pathak, K.G.Ayappa, S.N.Punnathanam. *J. Phys. Chem. C*, **116**, 23394 (2012)
131. Y.Byun, A.Coskun. *Chem. Mater*., **27**, 2576 (2015)
132. L.Mahmoudian, A.M.Rashidi, H.Dehghani, R.Rahighi. *Chem. Eng*., **304**, 784 (2016)
133. R.F.Cracknell, P.Gordon, K.E.Gubbins. *J. Phys. Chem*., **97**, 494 (1993)
134. M.E.Casco, M.Martínez-Escandell, K.Kaneko, J.Silvestre-Albero, F.Rodríguez-Reinoso. *Carbon*, **93**, 11 (2015)
135. C.Petit, J.Burress, T.J.Bandosz. *Carbon*, **49**, 563 (2011)
136. G.Ning, H.Wang, X.Zhang, C.Xu, G.Chen, J.Gao. *Particuology*, **11**, 415 (2013)
137. G.Srinivas, J.Burress, T.Yildirim. *Energy Environ. Sci*., **5**, 6453 (2012)
138. A.A.G.Blanco, A.F.Vallone, S.A.Korili, A.Gil, K.Sapag. *Microporous Mesoporous Mater*., **224**, 323 (2016)
139. A.W.Thornton, S.A.Furman, K.M.Nairn, A.J.Hill, J.M.Hill, M.R.Hill. *Microporous Mesoporous Mater*., **167**, 188 (2013)
140. X.-Q.Liu, Y.Xue, Z.-Y.Tian, J.-J.Mo, N.-X.Qiu, W.Chu, H.-P.Xie. *Appl. Surf. Sci*., **285**, 190 (2013)
141. H.Seema, K.C.Kemp, N.H.Le, S.-W.Park, V.Chandra, J.W.Lee, K.S.Kim. *Carbon*, **66**, 320 (2014)
142. Z.-Y.Sui, Y.-N.Meng, P.-W.Xiao, Z.-Q.Zhao, Z.-X.Wei, B.-H.Han. *ACS Appl. Mater. Interfaces*, **7**, 1431 (2015)
143. G.Ning, C.Xu, L.Mu, G.Chen, G.Wang, J.Gao, Z.Fan, W.Qian, F.Wei. *Chem. Commun*., **48**, 6815 (2012)
144. A.Ganesan, M.M.Shaijumon. *Microporous Mesoporous Mater*, **220**, 21 (2016)
145. M.P.Suh, H.J.Park, T.K.Prasad, D.-W.Lim. *Chem. Rev*., **112**, 782 (2011)
146. J.-R.Li, J.Sculley, H.-C.Zhou. *Chem. Rev*., **112**, 869 (2011)
147. Y.Peng, V.Krungleviciute, I.Eryazici, J.T.Hupp, O.K.Farha, T.Yildirim. *J. Am. Chem. Soc*., **135**, 11887 (2013)
148. I.Senkovska, S.Kaskel. *Microporous Mesoporous Mater*., **112**, 108 (2008)
149. C.Petit, T.J.Bandosz. *Adv. Funct. Mater*., **20**, 111 (2010)
150. C.Petit, T.J.Bandosz. *Adv. Funct. Mater*., **21**, 2108 (2011)
151. F.Xu, Y.Yu, J.Yan, Q.Xia, H.Wang, J.Li, Z.Li. *Chem. Eng*., **303**, 231 (2016)
152. W.Huang, X.Zhou, Q.Xia, J.Peng, H.Wang, Z.Li. *Ind. Eng. Chem. Res*., **53**, 11176 (2014)
153. S.Liu, L.Sun, F.Xu, J.Zhang, C.Jiao, F.Li, Z.Li, S.Wang, Z.Wang, X.Jiang. *Energy Environ. Sci*., **6**, 818 (2013)
154. X.Zhou, W.Huang, J.Miao, Q.Xia, Z.Zhang, H.Wang, Z.Li. *Chem. Eng*., **266**, 339 (2015)
155. J.Sreńscek-Nazzal, W.Kamińska, B.Michalkiewicz, Z.C.Koren. *Ind. Crop. Prod*., **47**, 153 (2013)
156. J.Cai, J.Qi, C.Yang, X.Zhao. *ACS Appl. Mater. Interfaces*, **6**, 3703 (2014)
157. L.Giraldo, J.Moreno-Piraján. *Mater. Sci. Appl*., **2**, 331 (2011)
158. N.Bagheri, J.Abedi. *Chem. Eng. Res. Des*., **89**, 2038 (2011)
159. F.Gholipour, M.Mofarahi. *J. Supercrit. Fluids*, **111**, 47 (2016)
160. N.Kostoglou, G.Constantinides, G.Charalambopoulou, T.Steriotis, K.Polychronopoulou, Y.Li, K.Liao, V.Ryzhkov, C.Mitterer, C.Rebholz. *Thin Solid Films*, **596**, 242 (2015)
161. B.Girek, W.Sliwa. *J. Incl. Phenom. Macrocycl. Chem*., **82**, 283 (2015)
162. D.Nuvoli, L.Valentini, V.Alzari, S.Scognamillo, S.B.Bon, M.Piccinini, J.Illescas, A.Mariani. *J. Mater. Chem*., **21**, 3428 (2011)
163. M.Lotya, P.J.King, U.Khan, S.De, J.N.Coleman. *ACS Nano*, **4**, 3155 (2010)
164. S.P.Economopoulos, G.Rotas, Y.Miyata, H.Shinohara, N.Tagmatarchis. *ACS Nano*, **4**, 7499 (2010)
165. T.Skaltsas, N.Karousis, H.-J.Yan, C.-R.Wang, S.Pispas, N.Tagmatarchis. *J. Mater. Chem*., **22**, 21507 (2012)
166. A.Ghosh, K.V.Rao, S.J.George, C.N.R.Rao. *Chem. – Eur. J*., **16**, 2700 (2010)
167. X.Zhang, Y.Feng, S.Tang, W.Feng. *Carbon*, **48**, 211 (2010)
168. Q.Yang, X.Pan, F.Huang, K.Li. *J. Phys. Chem. C*, **114**, 3811 (2010)
169. W.Auwärter, D.Écija, F.Klappenberger, J.V.Barth. *Nat. Chem*., **7**, 105 (2015)
170. G.Rojas, X.Chen, C.Bravo, J.-H.Kim, J.-S.Kim, J.Xiao, P.A.Dowben, Y.Gao, X.C.Zeng, W.Choe, A.Enders. *J. Phys. Chem. C*, **114**, 9408 (2010)
171. T.E.Shubina, H.Marbach, K.Flechtner, A.Kretschmann, N.Jux, F.Buchner, H.-P.Steinrück, T.Clark, J.M.Gottfried. *J. Am. Chem. Soc*., **129**, 9476 (2007)
172. T.A.Jung, R.R.Schlittler, J.K.Gimzewski. *Nature (London)*, **386**, 696 (1997)
173. T.Yokoyama, S.Yokoyama, T.Kamikado, Y.Okuno, S.Mashiko. *Nature (London)*, **413**, 619 (2001)
174. T.Yokoyama, S.Yokoyama, T.Kamikado, S.Mashiko. *J. Chem. Phys*., **115**, 3814 (2001)
175. C.X.Guo, Y.Lei, C.M.Li. *Electroanalysis*, **23**, 885 (2011)
176. M.A.Khaderbad, V.Tjoa, M.Rao, R.Phandripande, S.Madhu, J.Wei, M.Ravikanth, N.Mathews, S.G.Mhaisalkar, V.R.Rao. *ACS Appl. Mater. Interfaces*, **4**, 1434 (2012)
177. M.Jahan, Q.Bao, K.P.Loh. *J. Am. Chem. Soc*., **134**, 6707 (2012)
178. Q.Wang, J.Lei, S.Deng, L.Zhang, H.Ju. *Chem. Commun*., **49**, 916 (2013)
179. X.Zhang, L.Hou, A.Cnossen, A.C.Coleman, O.Ivashenko, P.Rudolf, B.J.van Wees, W.R.Browne, B.L.Feringa. *Chem. – Eur. J*., **17**, 8957 (2011)
180. J.-H.Chen, W.G.Cullen, C.Jang, M.S.Fuhrer, E.D.Williams. *Phys. Rev. Lett*., **102**, 236805 (2009)
181. U.Khan, H.Porwal, A.O Neill, K.Nawaz, P.May, J.N.Coleman. *Langmuir*, **27**, 9077 (2011)

182. T.Skaltsas, S.Pispas, N.Tagmatarchis. *Chem. – Eur. J.*, **19**, 9286 (2013)
183. J.Malig, A.W.I.Stephenson, P.Wagner, G.G.Wallace, D.L.Officer, D.M.Guldi. *Chem. Commun.*, **48**, 8745 (2012)
184. J.P.Mensing, T.Kerdcharoen, C.Sriprachuabwong, A.Wisitsoraat, D.Phokharatkul, T.Lomas, A.Tuantranont. *J. Mater. Chem.*, **22**, 17094 (2012)
185. G.Katsukis, J.Malig, C.Schulz-Drost, S.Leubner, N.Jux, D.M.Guldi. *ACS Nano*, **6**, 1915 (2012)
186. A.Castellanos-Gomez, B.J.van Wees. *Graphene*, **2**, 102 (2013)
187. C.F.Hermanns, K.Tarafder, M.Bernien, A.Krüger, Y.-M.Chang, P.M.Oppeneer, W.Kuch. *Adv. Mater.*, **25**, 3473 (2013)
188. M.Zhu, Z.Li, B.Xiao, Y.Lu, Y.Du, P.Yang, X.Wang. *ACS Appl. Mater. Interfaces*, **5**, 1732 (2013)
189. J.Geng, H.-T.Jung. *J. Phys. Chem. C*, **114**, 8227 (2010)
190. Y.Xu, L.Zhao, H.Bai, W.Hong, C.Li, G.Shi. *J. Am. Chem. Soc.*, **131**, 13490 (2009)
191. T.-X.Ye, S.-L.Ye, D.-M.Chen, Q.-A.Chen, B.Qiu, X.Chen. *Spectrochim. Acta, Part A*, **86**, 467 (2012)
192. S.Wan, J.Pu, X.Zhang, L.Wang, Q.Xue. *Appl. Phys. Lett.*, **102**, 011603 (2013)
193. P.Guo, P.Chen, M.Liu. *ACS Appl. Mater. Interfaces*, **5**, 5336 (2013)
194. A.I.Zvyagina, A.A.Shiryaev, A.E.Baranchikov, V.V.Chernyshev, Y.Yu.Enakieva, O.A.Raitman, A.A.Ezhov, I.N.Meshkov, D.A.Grishanov, O.S.Ivanova, Yu.G.Gorbunova, V.V.Arslanov, M.A.Kalinina. *New J. Chem.*, **41**, 948 (2017)
195. W.Auwärter, A.Weber-Bargioni, A.Riemann, A.Schiffrin, O.Gröning, R.Fasel, J.Barth. *J. Chem. Phys.*, **124**, 194708 (2006)
196. W.Auwärter, F.Klappenberger, A.Weber-Bargioni, A.Schiffrin, T.Strunskus, C.Wöll, Y.Pennec, A.Riemann, J.V.Barth. *J. Am. Chem. Soc.*, **129**, 11279 (2007)
197. F.Klappenberger, A.Weber-Bargioni, W.Auwärter, M.Marschall, A.Schiffrin, J.V.Barth. *J. Chem. Phys.*, **129**, 214702 (2008)
198. D.Heim, D.Ecija, K.Seufert, W.Auwärter, C.Aurisicchio, C.Fabbro, D.Bonifazi, J.V.Barth. *J. Am. Chem. Soc.*, **132**, 6783 (2010)
199. D.Heim, K.Seufert, W.Auwärter, C.Aurisicchio, C.Fabbro, D.Bonifazi, J.V.Barth. *Nano Lett.*, **10**, 122 (2009)
200. Z.Shi, N.Lin. *J. Am. Chem. Soc.*, **131**, 5376 (2009)
201. Y.Li, J.Xiao, T.E.Shubina, M.Chen, Z.Shi, M.Schmid, H.-P.Steinrück, J.M.Gottfried, N.Lin. *J. Am. Chem. Soc.*, **134**, 6401 (2012)
202. Z.Shi, N.Lin. *J. Am. Chem. Soc.*, **132**, 10756 (2010)
203. L.-A.Fendt, M.Stöhr, N.Wintjes, M.Enache, T.A.Jung, F.Diederich. *Chem. – Eur. J.*, **15**, 11139 (2009)
204. N.Wintjes, J.Hornung, J.Lobo-Checa, T.Voigt, T.Samuely, C.Thilgen, M.Stöhr, F.Diederich, T.A.Jung. *Chem. – Eur. J.*, **14**, 5794 (2008)
205. T.Yokoyama, T.Kamikado, S.Yokoyama, S.Mashiko. *J. Chem. Phys.*, **121**, 11993 (2004)
206. H.Spillmann, A.Kiebele, M.Stöhr, T.A.Jung, D.Bonifazi, F.Cheng, F.Diederich. *Adv. Mater.*, **18**, 275 (2006)
207. W.Auwärter, K.Seufert, F.Klappenberger, J.Reichert, A.Weber-Bargioni, A.Verdini, D.Cvetko, M.Dell Angela, L.Floreano, A.Cossaro, G.Bavdek, A.Morgante, A.P.Seitsonen, J.V.Barth. *Phys. Rev., B*, **81**, 245403 (2010)
208. A.Wiengarten, K.Seufert, W.Auwärter, D.Ecija, K.Diller, F.Allegretti, F.Bischoff, S.Fischer, D.A.Duncan, A.C.Papageorgiou, F.Klappenberger, R.G.Acres, T.H.Ngo, J.V.Barth. *J. Am. Chem. Soc.*, **136**, 9346 (2014)
209. L.Grill, M.Dyer, L.Lafferentz, M.Persson, M.Peters, S.Hecht. *Nat. Nanotechnol.*, **2**, 687 (2007)
210. L.Lafferentz, V.Eberhardt, C.Dri, C.Africh, G.Comelli, F.Esch, S.Hecht, L.Grill. *Nat. Chem.*, **4**, 215 (2012)
211. M.In't Veld, P.Iavicoli, S.Haq, D.B.Amabilino, R.Raval. *Chem. Commun.*, 1536 (2008)
212. S.Haq, F.Hanke, J.Sharp, M.Persson, D.B.Amabilino, R.Raval. *ACS Nano*, **8**, 8856 (2014)
213. O.Shoji, H.Tanaka, T.Kawai, Y.Kobuke. *J. Am. Chem. Soc.*, **127**, 8598 (2005)
214. M.C.O'Sullivan, J.K.Sprafke, D.V.Kondratuk, C.Rinfray, T.D.W.Claridge, A.Saywell, M.O.Blunt, J.N.O'Shea, P.H.Beton, M.Malfois, H.L.Anderson. *Nature (London)*, **469**, 72 (2011)
215. P.Järvinen, S.K.Hämäläinen, K.Banerjee, P.Häkkinen, M.Ijäs, A.Harju, P.Liljeroth. *Nano Lett.*, **13**, 3199 (2013)
216. S.Joshi, F.Bischoff, R.Koitz, D.Ecija, K.Seufert, A.P.Seitsonen, J.Hutter, K.Diller, J.I.Urgel, H.Sachdev, J.V.Barth, W.Auwärth. *ACS Nano*, **8**, 430 (2013)
217. J.Mao, H.Zhang, Y.Jiang, Y.Pan, M.Gao, W.Xiao, H.-J.Gao. *J. Am. Chem. Soc.*, **131**, 14136 (2009)
218. M.Bazarnik, J.Brede, R.Decker, R.Wiesendanger. *ACS Nano*, **7**, 11341 (2013)
219. K.Seufert, W.Auwärter, F.J.García de Abajo, D.Ecija, S.Vijayaraghavan, S.Joshi, J.V.Barth. *Nano Lett.*, **13**, 6130 (2013)
220. X.Qiu, C.Wang, Q.Zeng, B.Xu, S.Yin, H.Wang, S.Xu, C.Bai. *J. Am. Chem. Soc.*, **122**, 5550 (2000)
221. S.B.Lei, C.Wang, S.X.Yin, H.N.Wang, F.Xi, H.Liu, B.Xu, L.J.Wan, C.L.Bai. *J. Phys. Chem. B*, **105**, 10838 (2001)
222. B.Friesen, B.Wiggins, J.L.McHale, U. Mazur, K.W.Hipps. *J. Am. Chem. Soc.*, **132**, 8554 (2010)
223. S.Yoshimoto, T.Sawaguchi, W.Su, J.Jiang, N.Kobayashi. *Angew. Chem., Int. Ed.*, **119**, 1089 (2007)
224. J.Otsuki, Y.Komatsu, D.Kobayashi, M.Asakawa, K.Miyake. *J. Am. Chem. Soc.*, **132**, 6870 (2010)
225. R.van Hameren, P.Schön, A.M.van Buul, J.Hoogboom, S.V.Lazarenko, J.W.Gerritsen, H.Engelkamp, P.C.M.Christianen, H.A.Heus, J.C.Maan, T.Rasing, S.Speller, A.E.Rowan, J.A.A.W.Elemans, R.J.M.Nolte. *Science*, **314**, 1433 (2006)
226. L.Sanchez, R.Otero, J.M.Gallego, R.Miranda, N.Martin. *Chem. Rev.*, **109**, 2081 (2009)
227. S.Vijayaraghavan, D.Écija, W.Auwärter, S.Joshi, K.Seufert, A.P.Seitsonen, K.Tashiro, J.V.Barth. *Nano Lett.*, **12**, 4077 (2012)
228. S.Yoshimoto, E.Tsutsumi, Y.Honda, Y.Murata, M.Murata, K.Komatsu, O.Ito, K.Itaya. *Angew. Chem., Int. Ed.*, **116**, 3106 (2004)
229. D.Bonifazi, H.Spillmann, A.Kiebele, M.de Wild, P.Seiler, F.Cheng, H.-J.Güntherodt, T.Jung, F.Diederich. *Angew. Chem., Int. Ed.*, **43**, 4759 (2004)
230. S.Yoshimoto, Y.Honda, O.Ito, K.Itaya. *J. Am. Chem. Soc.*, **130**, 1085 (2008)
231. F.Sedona, M.Di Marino, M.Sambi, T.Carofiglio, E.Lubian, M.Casarin, E.Tondello. *ACS Nano*, **4**, 5147 (2010)
232. M.Li, S.Ishihara, Q.Ji, M.Akada, J.P.Hill, K.Ariga. *Sci. Technol. Adv. Mater.*, **13**, 053001 (2012)

233. J.Geng, Y.K.Ko, S.C.Youn, Y.-H.Kim, S.A.Kim, D.-H.Jung, H.-T.Jung. *J. Phys. Chem. C*, **112**, 12264 (2008)
234. M.B.M.Krishna, V.P.Kumar, N.Venkatramaiah, R.Venkatesan, D.N.Rao. *Appl. Phys. Lett.*, **98**, 081106 (2011)
235. H.Tang, H.Yin, J.Wang, N.Yang, D.Wang, Z.Tang. *Angew. Chem., Int. Ed.*, **125**, 5695 (2013)
236. R.Bera, S.Mandal, B.Mondal, B.Jana, S.Nayak, A.Patra. *ACS Sustain. Chem. Eng.*, **4**, 1562 (2016)
237. J.Geng, B.-S.Kong, S.B.Yang, H.-T.Jung. *Chem. Commun.*, **46**, 5091 (2010)
238. J.Malig, N.Jux, D.M.Guldi. *Acc. Chem. Res.*, **46**, 53 (2012)
239. S.Zhang, S.Tang, J.Lei, H.Dong, H.Ju. *J. Electroanal. Chem.*, **656**, 285 (2011)
240. M.B.M.Krishna, N.Venkatramaiah, R.Venkatesan, D.N.Rao. *J. Mater. Chem.*, **22**, 3059 (2012)
241. A.Wang, W.Yu, Z.Huang, F.Zhou, J.Song, Y.Song, L.Long, M.P.Cifuentes, M.G.Humphrey, L.Zhang, J.Shao, C.Zhang. *Sci. Rep.*, **6**, 23325 (2016)
242. C.-W.Kung, Y.-S.Li, M.-H.Lee, S.-Y.Wang, W.-H.Chiang, K.-C.Ho. *J. Mater. Chem. A*, **4**, 10673 (2016)
243. C.Su, K.P.Loh. *Acc. Chem. Res.*, **46**, 2275 (2012)